MINISTERE DE L'ENSEIGNEMENT SUPERIEUR ET DE LA RECHERCHE SCIENTIFIQUE
Felix houphouet-boigny university

Nº: 666

UNITE DE FORMATION ET DE RECHERCHE SCIENCES DES STRUCTURES DE LA MATIERE ET DE TECHNOLOGIE

RÉPUBLIQUE DE CÔTE D'IVOIRE
UNION - DISCIPLINE - TRAVAIL
RWTH Aachen University

SPONSORED BY THE

MASTER IN RENEWABLE ENERGY AND CLIMATE CHANGE

SPECIALITY: GREEN HYDROGEN/ GEORESOURCES

MASTER THESIS

Subject/Topic:

Five decades (1965-2014) of CLM5, ERA5 and GLDAS groundwater recharge in Africa with implications for green hydrogen production

Presented September, 28th 2023 by:

Helder António Alfredo Mutna

Jury members:

KOUADIO Yves	**President**	Full Professor	UFHB
KACOU Modeste	**Examinator**	Senior Lecturer	UFHB
FASSINOU Wanignon Ferdinand	**Director**	Senior Lecturer	UFHB
Harrie-Jan Hendricks-Franssen	**Co- Director**	Full Professor	FJZ

Academic year 2022-2023

ACKNOWLEDGEMENTS

The successful accomplishment of this scientific work has been made possible through the dedicated efforts of numerous organizations and individuals. I would like to express my heartfelt gratitude to the following individuals and institutions: First and foremost, I extend my sincere appreciation to the Federal Ministry of Education and Research (BMBF) for their invaluable support of this significant program in Africa, particularly within the ECOWAS region.

I am deeply thankful to the West African Science Service Centre on Climate Change and Adapted Land Use (WASCAL) for their exceptional management of the program. Special thanks go to Professor Rabani Adamou, the Director of WASCAL - Niger, and his entire team for their comprehensive guidance throughout both the first and second semesters of the program. Likewise, I extend my gratitude to the entire WASCAL Côte d'Ivoire team, including Professor KOUASSI Konan Edouard, the Director, Professor Koné N'golo Abdoulaye, the Deputy Director, Doctor FASSINOU W. Ferdinand, the H2 program Coordinator, and the Scientific Coordinator. Their professional guidance during the third semester and the provided facilities were immensely valuable.

I am indebted to the Vice Chancellor of Aachen University and the head of the Institute of Bio- and Geosciences – Agrosphere (IBG-3) for granting me the opportunity to undertake my internship at their esteemed institution. My heartfelt thanks go to my supervisors. Professor Harrie-Jan Hendricks-Franssen's extensive expertise and professionalism were instrumental throughout the course of this work. Dr. FASSINOU Wanignon Ferdinand's dedicated support from the outset is deeply appreciated. I am particularly grateful to my co-supervisors, Dr. Bagher Bayat and Bamidele Oloruntoba, for their continuous availability, enthusiasm, and the cohesive team spirit they fostered among us. I extend my sincere gratitude to all the jury members, including President KOUADIO Yves, Examiner KACOU Modeste, Director FASSINOU Wanignon Ferdinand, and Co-Director Harrie-Jan Hendricks-Franssen, for their invaluable contributions to the improvement of this master's thesis.

Finally, I want to express my gratitude to my fellow classmates, with a special mention to Souleymane Fanta Konaté, Yoda Houssokri Zounogo Wahabou, Amadou Barry, and Abdellah Kéziré, for their unwavering support that significantly contributed to the successful completion of this program.

ABSTRACT

This study investigates the spatiotemporal distribution of decadal mean groundwater recharge (GWR) across Africa from 1965 to 2014. The analysis employs the Community Land Model version 5 (CLM5) as the reference dataset, alongside the European Reanalysis dataset version 5 (ERA5-Land) and Global Land Data Assimilation System version 2 (GLDAS_2.0) as additional dataset. Groundwater recharge calculations utilize a water balance approach, revealing mean decadal recharge rates of 45.5 mm/year for CLM5, 129.9 mm/year for ERA5-Land, and 155.4 mm/year for GLDAS. Remarkably, regions such as Central Africa, Central-East Africa, West Africa, South-East Africa, and North-East Africa (including Ethiopia) demonstrate substantial groundwater availability. Fascinatingly, a strong similarity emerges between Precipitation and Evapotranspiration across the models. Specifically, the average annual precipitation stands at 644.6 mm for CLM5, 627.2 mm for GLDAS, and 691.6 mm for ERA5-Land. Correspondingly, the annual evapotranspiration rates are 480.8 mm for CLM5, 462.8 mm for GLDAS_2.0, and 526.7 mm for ERA5. Statistical analyses establish a noteworthy correlation between CLM5 and GLDAS_2.0. This correlation underscores the reliability of the models in assessing groundwater recharge. The identification of regions with elevated groundwater recharge potential lays a crucial foundation for informed decision-making in the establishment of green hydrogen projects. Moreover, it emphasizes the indispensable role of accurate hydrological modelling in shaping sustainable water resource strategies for advancing energy sustainability. In moving forward, collaboration between stakeholders, policymakers, and researchers is pivotal. Such partnerships can facilitate the assessment of the feasibility of green hydrogen projects in areas with significant recharge potential. This assessment must holistically consider both groundwater availability and the broader landscape of renewable energy resources. This study's findings hold substantial implications for steering environmentally conscious energy initiatives and ensuring harmonious resource management.

Keywords: groundwater recharge; green hydrogen; Climate change; renewable energy; sustainable development.

RÉSUMÉ

Cette étude porte sur la répartition spatio-temporelle de la recharge décennale moyenne des eaux souterraines (RES) à travers l'Afrique de 1965 à 2014. L'analyse utilise le Modèle Communautaire de Terrain version 5 (CLM5) en tant que jeu de données de référence, ainsi que le jeu de données de Réanalyse Européenne version 5 (ERA5-Land) et le Système Global d'Assimilation des Données Terrestres version 2 (GLDAS_2.0) en tant que jeux de données additionnels. Les calculs de recharge des eaux souterraines utilisent une approche de bilan hydrique, révélant des taux moyens de recharge décennale de 45,5 mm/an pour CLM5, 129,9 mm/an pour ERA5-Land et 155,4 mm/an pour GLDAS. De manière remarquable, des régions telles que l'Afrique centrale, l'Afrique Centre-Est, l'Afrique de l'Ouest, l'Afrique du Sud-Est et l'Afrique du Nord-Est (y compris l'Éthiopie) démontrent une disponibilité substantielle en eaux souterraines. Il est intéressant de noter une forte similitude entre les précipitations et l'évapotranspiration à travers les modèles. Plus spécifiquement, la précipitation annuelle moyenne s'élève à 644,6 mm pour CLM5, 627,2 mm pour GLDAS et 691,6 mm pour ERA5-Land. De même, les taux annuels d'évapotranspiration sont de 480,8 mm pour CLM5, 462,8 mm pour GLDAS_2.0 et 526,7 mm pour ERA5-Land. Les analyses statistiques établissent une corrélation significative entre CLM5 et GLDAS_2.0. Cette corrélation souligne la fiabilité des modèles dans l'évaluation de la recharge des eaux souterraines. L'identification des régions à fort potentiel de recharge des eaux souterraines pose des bases cruciales pour la prise de décision éclairée dans la mise en place de projets d'hydrogène vert. De plus, cela met en avant le rôle indispensable de la modélisation hydrologique précise dans la formulation de stratégies durables pour l'avancement de la durabilité énergétique. Pour aller de l'avant, la collaboration entre les parties prenantes, les décideurs et les chercheurs est essentielle. De telles collaborations peuvent faciliter l'évaluation de la faisabilité des projets d'hydrogène vert dans les zones à fort potentiel de recharge. Cette évaluation doit prendre en compte de manière holistique à la fois la disponibilité des eaux souterraines et le panorama plus large des ressources en énergie renouvelable. Les conclusions de cette étude ont des implications substantielles pour orienter des initiatives énergétiques respectueuses de l'environnement et assurer une gestion harmonieuse des ressources.

Mots-clés : recharge des eaux souterraines ; hydrogène vert ; changement climatique ; énergie renouvelable ; développement durable.

TABLE OF CONTENTS

ACRONYMS and ABBREVIATIONS

BF	BaseFlow
CAB	Congo Air Boundary
CAF	Central Africa
CEAF	Central-East Africa
CESM	Community Earth System Model
CLM5	Community Land Model version 5
CMB	Chloride Mass Balance
CRU	Climate Research Unit
ECMWF	European Centre for Medium-Range Weather Forecasts
Eq.	Equation
ERA5-Land	European ReAnalysis dataset version 5
ET	Evapotranspiration
Fig.	Figure
GLDAS_2.0	Global Land Data Assimilation System version 2.0
GPCC	Global Precipitation Climatology Centre
GSFC	Goddard Space Flight Center
GSWP3	Third Global Soil Wetness Project
GWLFT	Groundwater-Level Fluctuation Techniques
GWMs	Groundwater Models
GWR	Groundwater Recharge
ITCZ	Intertropical Convergence Zone
ITD	Intertropical Discontinuity
KGE	Kling-Gupta Efficiency
LTA	Long-Term Average
MED	Mediterranean
NASA	National Aeronautics and Space Administration
NCEP	National Centers for Environmental Prediction
NEAF	North-East Africa
NOAA	National Oceanic and Atmospheric Administration
PT	Precipitation

Q	Surface runoff
PGMF	Princeton Global Meteorological Forcing
RMSD	Root Mean Squared Distance
RMSE	Root Mean Square Error
SAH	Sahara
SEAF	South-East Africa
SWAF	South-West Africa
TCA	Triple collocation analysis
WAF	West Africa
WBA	Water Balance Analysis

LIST OF FIGURES

LIST OF TABLES

GENERAL INTRODUCTION

Global reliance on groundwater as a vital freshwater source is unparalleled, serving as a cornerstone for drinking water, agriculture, and industry (West et al., 2023). In contrast, Africa holds only 9% of the world's renewable freshwater resources, estimated at 43,750 km^3/year (Springer et al., 2023). Understanding the dynamics of groundwater recharge (GWR) across time and space is paramount for ensuring groundwater security (MacDonald et al., 2021).

A comprehensive assessment of GWR's long-term average (LTA) diffuse process, the process of recharge that occurs over a wide area and is derived from precipitation or irrigation (Keese et al., 2005), was achieved through Water GAP (Global Hydrology Model WGHM) (Döll and Fiedler, 2008). Historically, GWR studies have notably focused on Southern Africa, North Africa, and the Sudano-Sahel of West Africa (MacDonald et al., 2021). However, substantial gaps persist in detailed groundwater information in many African regions (Adelana et al., 2009).

Despite the emphasis on arid and semi-arid regions (Hendrickx, 1992; Edmunds and Gaye, 1994; Kumar, 1997; Scanlon et al., 2006; Taylor et al., 2013; Seddon, 2019; Xu and Beekman, 2019), limited studies cover tropical environments (Wang et al., 2010). Accurately estimating GWR remains challenging due to its integration of various uncertain components, especially in semi-arid areas (Reinecke et al., 2021). Among methods, the Chloride Mass Balance approach prevails but necessitates better monitoring of chloride input (Scanlon et al., 2006).

Systematic groundwater monitoring in Africa remains rare, prompting the exploration of modeling to provide broader insights, especially at a continental scale (Bonsor et al., 2018). The past decade has seen considerable African GWR research (Chung et al., 2016), including quantifying GWR volumes (MacDonald, 2021), spatiotemporal variability assessments (Scanlon, 2022) and groundwater management opportunities (Gaye and Tindimugaya, 2018).

In 2013, the African Union launched "Agenda 2063," aiming to position the continent as a future global force (AbouSeada and Hatem, 2022). Africa's potential in renewable energy is widely acknowledged, offering solutions for energy needs, economic growth, and global CO_2 reduction goals. Notably, producing large-scale green hydrogen is pivotal in decarbonization efforts. Research indicates that embracing green hydrogen fuels and anticipating heightened demand could significantly cut emissions, crucial for realizing Net Zero Emissions (Winter et al., 2022). Producing 2.3 Gt of hydrogen would require 20.5 Gt (or 20.5 billion m^3) of freshwater annually, which is only a small fraction of Earth's available freshwater (Beswick et al., 2021). Africa's groundwater reserves are substantial, about 0.66 million km^3, dwarfing the water stored in its lakes by 20-fold (MacDonald et al., 2021; Springer et al., 2023). These immense potential positions groundwater as a viable, feasible source for green hydrogen production. Despite this, no study has yet explored GWR across Africa for its implications in green hydrogen. Our study fills this gap by focusing on this aspect.

Employing the water balance method, we ascertain GWR, utilizing models like the Community Land Model [ver. 5] (CLM) (Lawrence et al. 2019). Additionally, the Global Land Data Assimilation System version 2 (GLDAS_2.0) and the European ReAnalysis dataset (Era5-Land) are used ((Muñoz Sabater, 2019; Rodell et al., 2004) This study spans half a century (1965-2014) across Africa, encompassing GWR analysis, water balance component examination, and spatiotemporal pattern investigation from these models.

The insights gained from this research are valuable as they can identify regions where the simulated potential GWR from CLM5, ERA5-Land, and GLDAS_2.0 align well and can be utilized for establishing green hydrogen production projects. Furthermore, the study highlights the limitations inherent in using simulated datasets for these purposes. Ultimately, our findings contribute to a better understanding of groundwater resources and their potential for sustainable green hydrogen production in Africa.

The general introduction provides background information and clearly states the objective of the study. The first chapter of this thesis offers a comprehensive overview of the general concept of groundwater recharge (GWR) and identifies the key factors influencing it. Chapter two delves into the methodology employed and describes the dataset utilized. Moving on to chapter three, the results are presented and discussed, including comparisons among different datasets. Finally, the study's main conclusions are discussed, and potential avenues for future research are outlined.

Chapter 1: LITERATURE REVIEW

Chapter 1: LITERATURE REVIEW

INTRODUCTION

In the present chapter, we embark on an extensive exploration of the principal concepts and determinants that exert influence upon GWR. Our exposition is meticulously derived from a comprehensive review of the existing literature. The gamut of factors encompassed in this deliberation comprises, but is not limited to, meteorological variables such as precipitation, the intricate processes of evapotranspiration, but also the soil types, geological formations, geomorphological features, and the nuances of topographical variations. Additionally, we delve into the overarching significance of groundwater within the African context and expound upon the critical dimension of groundwater security within the region. This discourse serves a dual purpose: to provide a comprehensive elucidation of the extant research landscape and to set the stage for a seamless transition into subsequent chapters, thereby guiding the reader through the forthcoming analytical and empirical investigations.

1.1 CONCEPTS OF GROUNDWATER RECHARGE

During the early 20th century, Rushton and Ward (1979) defined GWR as the amount of surface water that reaches the permanent water table through direct contact in the riparian zone or downward percolation through the overlying zone of aeration. Danielopol et al. (2003) and Abiye (2016) have conceptually distinguished three types of recharges: localized recharges, which involve the accumulation of precipitation in surface water bodies followed by concentrated infiltration and percolation through the unsaturated zone to a groundwater body; and direct recharges, which entail direct infiltration of precipitation and subsequent percolation through the unsaturated zone to a groundwater body. GWR can occur through diffuse or focused mechanisms (MacDonald et al., 2021). Diffuse recharging occurs across a wide region when precipitation percolates through the soil to the water table. Focused recharge, on the other hand, takes place in areas where water leaks from surface water sources such as lakes, rivers, wetlands, and wadis, and it tends to become more prevalent in arid regions (Cuthbert et al., 2019). Focused recharge can be either discrete, where a single river or water body provides significant local recharge, or widely spread, where ephemeral rivers, depressions, or rock fractures are prevalent across a large area and contribute to regional recharge, as seen in portions of the Sahel (MacDonald et al., 2021). Obuobie (2008) highlighted a range of methods to estimate groundwater recharge (GWR) across Africa. These methods, including baseflow estimation (BF), soil physics techniques, tracers, groundwater-level fluctuation (GWLF), water balance analysis (WBA), and groundwater models, aim to replicate actual recharge processes. GWR is influenced by factors such as precipitation rate, soil moisture, geology, vegetation, land use, and aquifer properties (Obuobie, 2008).

1.2 FACTORS CONTROLLING GROUNDWATER RECHARGE

1.2.1 PRECIPITATION

The distribution of precipitation (PT) across Africa (Fig. 1) significantly influences groundwater recharge (GWR). PT patterns are characterized by a clear trend. Equatorial regions near the Gulf of Guinea and Mount Cameroon receive substantial rainfall, can exceeding 4000 mm annually (Gaye and Tindimugaya, 2018). However, as one moves northwards and southwards from these equatorial areas, the amount of PT gradually decreases, particularly towards the Sahara and the Kalahari. This trend is associated with the influence of mid-latitude westerlies, frontal systems, and convergence zones that contribute to precipitation in Africa (Hulme, 1992b).

This gradual decline in PT is influenced by various climatic factors. The Intertropical Discontinuity (ITD) and the Intertropical Convergence Zone (ITCZ) play a crucial role in PT distribution. The ITD represents the boundary between moist tropical air and drier subtropical air, creating a region of distinct changes in weather patterns. The ITCZ, on the other hand, is a low-pressure belt around the equator where trade winds converge, leading to ascending moist air and heavy rainfall (Hulme, 1992a; IPCC, 2007). Furthermore, the Congo Air Boundary (CAB) is a notable feature affecting precipitation. The CAB is a region of convergence between moist maritime air from the Atlantic Ocean and drier continental air from the African interior. This convergence results in enhanced cloud formation and precipitation over Central Africa (Nicholson, 2000; Vizy and Cook, 2002).

PT in Africa is generally associated with the mid-latitude westerlies, including the associated frontal systems, and especially convergence zones (Hulme, 1992b). The rainiest places are the poleward extremes, where mean annual PT ranges from 800 to 1200 mm, and the equatorial zone, where it ranges from 1200 to 2000 mm. Additionally, abundant PT is observed over the highland regions of Eastern Africa, Cameroon, and Nigeria, as well as the coastal areas of Liberia, Sierra Leone, and Guinea (Nicholson, 2000).

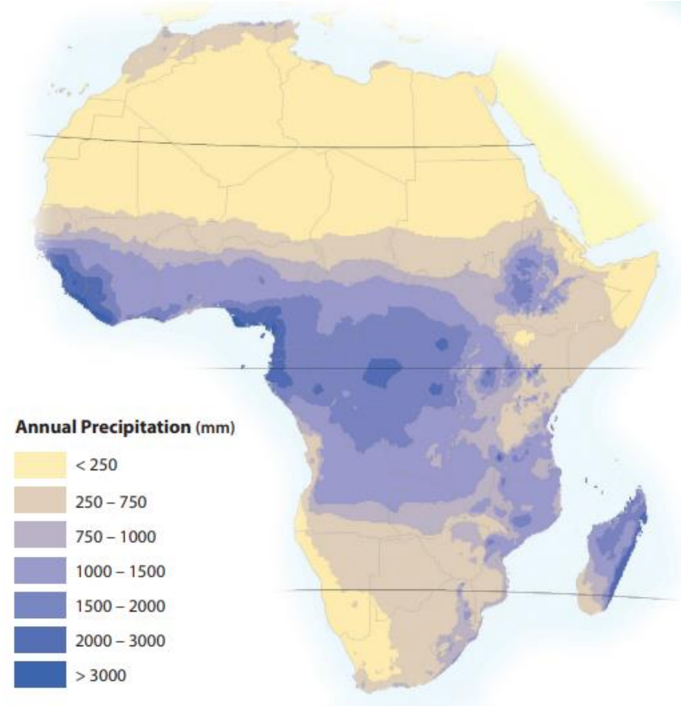

Figure 1. The pattern of mean annual precipitation, millimetres of rainfall, and the water equivalent of snowfall (European Commission. Joint Research Centre., 2013a)

1.2.2 EVAPOTRANSPIRATION

Evapotranspiration (ET), the process of transferring water from the land surface to the atmosphere, plays a pivotal role in the climate system. It intricately connects the water, energy, and carbon cycles (Shi et al., 2013). Over the course of a year, ET over land returns approximately 60% of precipitation (PT) that falls on land back into the atmosphere. This makes it the second-largest factor in the terrestrial water cycle, trailing only behind (Oki and Kanae, 2006).

ET's dynamics are influenced by the interplay of soil moisture availability and atmospheric moisture demand. Particularly notable is the robust relationship between evapotranspiration, temperature, and precipitation during the transition between wet (monsoonal) and dry climate regimes in moisture-limited sub-tropical regions (Marshall et al., 2012).

Africa, situated close to the Equator, encounters discernible temperature trends due to climate change. This continent receives copious amounts of radiation and has experienced accelerated warming (at a rate surpassing the global average). As demonstrated by Zeng et al (2012), the global mean annual ET for 1982–2009 was about 604 mm/year (ranging from 558 mm/year to 650 mm/year).

Teklebirhan et al (2012) delved into the Illala Catchment in Northern Ethiopia, employing the WetSpass Modelling Method to estimate GWR, ET, and surface runoff (Q). Their findings revealed a loss of around 440 mm of water through ET, constituting 81% of the annual PT. This underscores ET's predominant role in the water budget, attributed to heightened radiation and arid winds. Notably, about 79% of the total annual ET occurs during the summer season, with the remaining 21% released in winter.

Overall, Africa's GWR is significantly impacted by elevated ET levels, which stem from factors such as intense solar radiation, vegetation density, soil characteristics, and more.

1.2.3 SOIL TYPE

The type and properties of soil exhibit lateral and vertical variations from one place to another. The process of percolation and infiltration is closely linked to soil type (Balek, 1988). Saturated hydraulic conductivity (Ksat) is a measure of how easily water can flow through saturated soil under the influence of gravity. It represents the ability of the soil to transmit water and is influenced by various soil properties, including particle size distribution, porosity, and structure. Soils with higher Ksat values allow water to move more rapidly, while soils with lower Ksat values restrict water movement (Gee and Or, 2002).

Different soil types have varying levels of Ksat due to their distinct particle sizes and arrangements. Sandy soils, for instance, typically have larger particles and larger pore spaces between particles. This results in higher Ksat values and allows water to flow more easily through the soil. On the other hand, clay soils have smaller particles and smaller pore spaces, leading to lower Ksat values and slower water movement (Bouma, 1989; Saxton and Rawls, 2006). Argillaceous soils, which often serve as aquitards capable of storing water during the wet season, slow down recharge. Conversely, areas with crystalline rocks or permeable soil, combined with high rainfall, create ideal conditions for recharge (Abdullateef et al., 2021).

In the arid regions of Africa, the most prevalent soil types are sand dunes and shallow to deep gravelly soils classified as Entisols. Entisols are soils of recent origin developed in unconsolidated parent material, typically characterized by a single horizon, known as the A horizon (University of Idaho, 2023).

The Sudanian Zone South of the Sahara and the semiarid border of Southern Africa are predominantly occupied by Alfisols, which are moderately leached soils with relatively high native fertility. Arid-region Mollisols, which are soft soils found in grassland ecosystems, are limited to the Northwest coast and are sparsely distributed. Vertisols, clay-rich soils that shrink and swell with changes in moisture content, play a significant role as secondary soils in a few soil associations, particularly near the southern edge of the Sahara (Dregne, 1976).

1.2.4 GEOLOGY

Most of Africa consists of stable, ancient plateaus, with lower elevations in the North and West and higher elevations in the south and east (Adelana et al., 2009). A significant portion of Africa's groundwater, around 30%, is found within fractures and weathered zones that are part of complex geological formations. Due to the intricate geology, understanding the occurrence and movement of groundwater is highly challenging (Gaye and Tindimugaya, 2018). Macdonald et al. (2009), developed a simplified hydrogeological map for Africa (Fig.2b), categorizing four geological units where groundwater is likely to occur in a similar manner: Precambrian basement rocks, volcanic rocks, unconsolidated sediments, and consolidated sedimentary rocks. Heterogeneous Precambrian basement covers approximately 34% of the land area, followed by consolidated sedimentary rocks (37%), unconsolidated sediments (25%), and volcanic rocks (4%) (Adelana et al., 2009). Nearly 50% of Africa exhibits localized and shallow occurrences of groundwater, primarily confined to unconsolidated rocks near the surface (MacDonald and Davies, 2000).

1.2.4.1 Precambrian basement rocks

Within the entire continent, Precambrian crystalline rocks underlie the land. In the arid regions of Africa, these rocks are exposed across approximately a quarter to a third of the land surface (Dregne, 1976). These crystalline rocks consist of igneous and metamorphic formations that are more than 550 million years old. Groundwater in negligible quantities is found in unweathered and non-fractured basement rocks. However, substantial aquifers are formed within the weathered overburden and fractured bedrock (Wright, 1992).

1.2.4.2 Volcanic rocks

Volcanic rocks, constituting 4% of Africa's geographical surface, are predominantly located in East and Southern Africa. Despite their limited size, they have the potential to form significant aquifer systems, which is particularly noteworthy considering that they underlie many of Africa's poorest and most drought-stricken regions. The groundwater potential of volcanic rocks varies significantly due to the complexity of the underlying geology (Macdonald et al., 2009).

1.2.4.3 Unconsolidated sediments

Unconsolidated sediments play a significant role in forming some of Africa's most productive aquifers, covering approximately 25% of the continent's territory. It is important to note that this estimate likely underestimates their true significance, as the map only represents the thickest and most extensive deposits. Furthermore, unconsolidated sediments are also prevalent in numerous river valleys across Africa (Guiraud, 1988).

1.2.4.4 Consolidated sedimentary rocks

Consolidated sedimentary rocks, particularly extensive sandstone basins, possess a significant groundwater storage capacity. However, in arid regions, a substantial portion of the groundwater may be non-renewable as it was replenished during periods of higher rainfall in the past. The permeability of sedimentary rocks can vary greatly, ranging from low permeability mudstone and shale to higher permeability sandstones and limestones (MacDonald and Davies, 2000).

1.2.5 Geomorphology and Topography

In GWR, topography and geomorphology play a significant role. Topography, which is a key component of geomorphology, influences various factors such as groundwater recharge, flow rates, and surface run-off (Mulyadi et al., 2020). The topographical characteristics of major geomorphic regions in Africa (Fig. 2a) vary locally based on factors like rock composition and the effects of climatic changes (King, 1978). In Africa, higher tablelands are typically found in the East and South, gradually decreasing in altitude towards the West and North. The Atlas Mountain Range is separated and isolated by a depressed basin in the South. The high grounds of Hoggar and Tibesti consist of volcanic material and are situated on large elevated areas. The Ethiopian highlands, characterized by a rugged mountain mass, represents the largest continuous high-altitude area on the entire continent, with few surface areas descending below 1,500 meters. Lake Assal in Djibouti, located 156 meters below sea level, and the Danakil Depression in Ethiopia, situated 125 meters below sea level, are the lowest points on the African continent (European Commission. Joint Research Centre., 2013a).

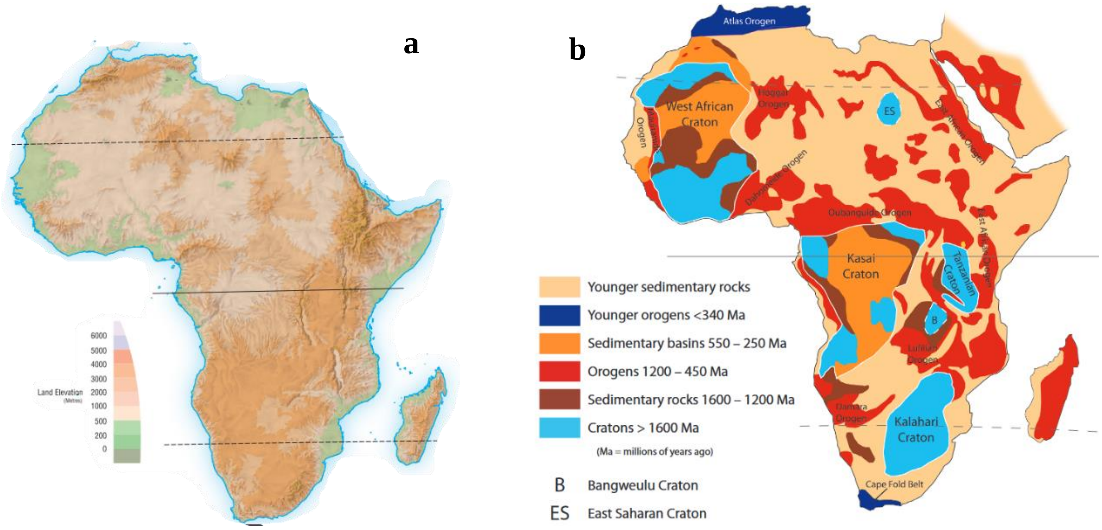

Figure 2. (a) Topographic map of land in Africa, and (b) simplified view of the geological structure and tectonic features of Africa (European Commission. Joint Research Centre., 2013)

1.3 AFRICA GROUNDWATER RESOURCES

Africa, characterized by its diverse climate, hydrology, and geology, presents one of the most variable and challenging hydrological environments among all inhabited continents (Adelana et al., 2008). The complex interplay of these factors results in diverse hydrogeological settings with numerous variations in groundwater resources, quality, accessibility, quantity, and renewability (Macdonald et al., 2009). Groundwater resources in Africa (Fig.3) remain poorly monitored and understood compared to other continents (MacDonald, 2012). Although continent-wide datasets on water resources exist, primarily based on remote sensing data or global model outputs (Wijnen et al., 2018), it is estimated that Africa's groundwater volume is approximately 0.66 million km^3, which is 20 times greater than the freshwater stored in African lakes (MacDonald et al., 2021; Springer et al., 2023). Notably, a significant portion of Africa's groundwater storage is concentrated in North African countries such as Libya, Algeria, Sudan, Egypt, and Morocco (MacDonald et al., 2012).

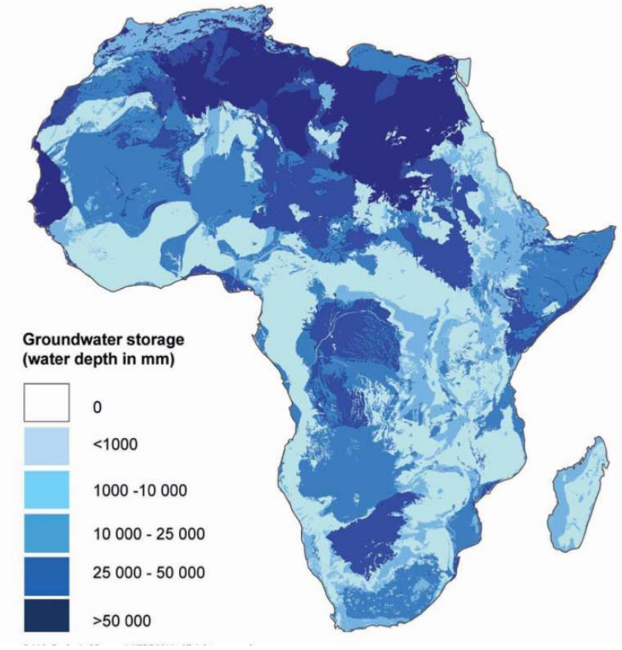

Figure 3. Map of groundwater storage in Africa (MacDonald et al., 2012)

1.4 THE IMPORTANCE OF GROUNDWATER IN AFRICA

Groundwater, which accounts for 36% of the world's drinking water supply and nearly 42% of irrigation water, is the largest accessible store of freshwater globally (Taylor et al., 2013). However, current statistics reveal that 1.1 billion people lack access to improved water supplies and 2.6 billion people lack adequate sanitation worldwide (Moe and Rheingans, 2006). In Africa, approximately 418 million people still lack even a basic level of drinking water service, 779 million lack basic sanitation services (UNICEF, 2022). Understanding the spatiotemporal patterns of groundwater and its driving factors at the continental scale is crucial for the sustainable management of water resources (Huang et al., 2021). Groundwater, being the largest water resource in Africa, has the potential to alleviate surface water scarcity, mitigate drought-related shocks, and support ecosystem health and human adaptation to climate variability and change (Reinecke et al., 2021; Wijnen et al., 2018). The future development of Africa, including areas such as irrigated agriculture, urban and rural water security, and drought resilience, is expected to increasingly depend on groundwater. Consequently, there will be a significant increase in demand for these resources.

1.5 GROUNDWATER SECURITY IN AFRICA

Adaptation to climate change remains a significant concern for Africa as historical data indicates that drought currently affects approximately 20% of the Earth's geographical surface. This percentage has risen to 28% and was expected to reach 35% by 2020 (Calow et al., 2010). Disturbingly, the area of the planet impacted by severe droughts has increased from 1% to 3% over the past decade, with projections indicating a further worsening of the situation (Burke et al., 2006). Climate change adaptation remains a critical issue for the continent. African countries have made little progress towards national water security. Despite these challenges, no African country has achieved an effective level of water security, indicating limited progress in this regard for the continent (Tsanni and Nakweya, 2022). However, the distribution of water resources in Africa provides a potential avenue for enhancing water security. Many countries with low recharge possess significant groundwater storage, while those with low storage experience high and regular recharge rates (MacDonald et al., 2021). The presence of aquifers plays a vital role in boosting water security as the substantial volume of stored groundwater within them can help mitigate the impact of drought on surface-water supplies (Foster and MacDonald 2014). Foster and MacDonald (2014) argue that groundwater storage should be given greater attention in determining water security, as it surpasses the consideration of yearly renewable resources alone to address physical water scarcity. This perspective challenges the prevailing emphasis on investing solely in-built reservoir infrastructure when advocating for improved water security. In summary, understanding and utilizing groundwater storage within aquifers is crucial for addressing water security concerns in Africa, especially in the face of increasing drought, climate change challenges, groundwater use in industry like green hydrogen production, and the associated increasing conflicts among different groundwater users.

PARTIAL CONCLUSION

In summation, our investigation underscores the pivotal roles played by precipitation and evapotranspiration in exerting a fundamental influence upon GWR dynamics across the African continent. Additionally, we acknowledge the substantial impact of soil types, owing to the varying hydraulic conductivity inherent to different soil classifications. It is noteworthy that Africa possesses a reservoir of groundwater resources, capable of providing essential drinking water services to communities. Our study accentuates the paramount importance of comprehending the spatiotemporal patterns of groundwater distribution and the factors that propel its variation on a continental scale.

Chapter 2: MATERIALS AND METHOD

Chapter 2: MATERIALS AND METHOD

INTRODUCTION

Within this chapter, we embark upon an elucidation of the materials harnessed in our study, accompanied by a meticulous exposition of the methodological deployed. A concise presentation of the fundamental equations employed for the calculation of error metrics is included herein. Furthermore, a comprehensive flowchart is delineated, elucidating the procedural intricacies underpinning the derivation of GWR within the CLM5 model.

2.1 MATERIALS

2.1.1 COMMUNITY LAND MODEL 5.0 (CLM5)

Version 5 of the open-source Community Land Model (CLM5) Table 1, is the land surface model component of the Community Earth System Model (CESM), and it simulates the soil, plant, atmosphere exchange processes (Lawrence et al., 2019). CLM5 enables the simulation of various processes, such as water exchange (evapotranspiration), energy exchange, carbon and nitrogen exchange between land and atmosphere, as well as the representation of soil and vegetation states like soil moisture, soil temperature, and leaf area index (CTSM, 2020). Developments for CLM5.0 build on the progress made in CLM4.5. Most major components of the model have been updated with particularly notable changes made to soil and plant hydrology, snow density, river modeling, carbon and nitrogen cycling and coupling, and crop modeling (CLM50_Tech_Note, 2018) The CLM5 surface data sets are created as in CLM4 and CLM4.5 but with updated methodology as described by Lawrence et al. (2019). Present-day global land cover descriptions are generated at 1-km resolution using updated versions of the data and methods used for CLM4 and CLM4.5 (Lawrence and Chase, 2007). The basis for the land cover description comes from MODIS land cover (MCD12Q1 v5.1), vegetation continuous fields (MOD44B v5.1), leaf area index (LAI) (MCD15A2 v5), and albedo (MCD43B3 v5) products for the years 2001–2015 (Lawrence et al., 2019). To run the CLM5 model, detailed atmospheric forcing data, including precipitation, shortwave and longwave incoming radiation, air temperature, wind speed, humidity, and surface air pressure is required. For this study, forcing data was obtained from the third Global Soil Wetness Project (GSWP3), providing 3-hourly forcing data at a global scale with a spatial resolution of 0.5˚ (GSWP3, 2014).

Table 1. Community Land Model version 5 (CLM5) model description (Lawrence et al., 2019; CTSM, 2023)

Aspect	Description
Model name	Community Land Model version 5 (CLM5)
Purpose	Land surface model for climate research and forecasting
Type	Process-based land surface model
Developers	Climate and Global Dynamics Laboratory, National Center for Atmospheric Research (NCAR)
Spatial Scale	Global
Components	Lower atmosphere, Land Surface, Vegetation, Hydrology, Biogeochemistry
Key Features	Detailed representation of land cover, vegetation types, soil properties, and hydrological processes
Temporal resolution	Hourly
Spatial Resolution	10 km
Hydrological Processes	Models surface runoff, evapotranspiration, soil moisture dynamics, and more
File format	NetCDF

2.1.2 EUROPEAN REANALYSIS DATASET (ERA5-Land)

ERA5-Land is the fifth generation of the European ReAnalysis dataset (Table 2), developed by the European Centre for Medium-Range Weather Forecasts (ECMWF). It has been produced to do over the land component of the ECMWF ERA5 climate reanalysis (Li et al., 2022). This dataset offers a consistent and enhanced view of land variable evolution over several decades, combining model data with global observations to create a complete and coherent dataset using the principles of physics (Muñoz Sabater, 2019). The production period for ERA5-Land spans from 1950 to the present (Muñoz Sabater et al., 2021). ERA5-Land boasts a high spatial resolution of 0.1 degrees (approximately 9 km) and a temporal resolution of one hour (Li et al., 2022).

These characteristics allow for the detailed representation of water and energy cycles over land throughout the production period, facilitating the analysis of trends and anomalies (Muñoz Sabater et al., 2021). Due to its exceptional temporal and spatial resolutions, ERA5-Land is driven by atmospheric forcing derived from ERA5 near-surface meteorology state and flux fields. The meteorological state fields are obtained from the lowest ERA5 model level (level 137), which is 10 m above the surface, and include air temperature, specific humidity, wind speed, and surface pressure (Muñoz-Sabater et al., 2021). The surface fluxes include downward shortwave and longwave radiation and liquid and solid total precipitation. These fields are interpolated from the ERA5 resolution of about 31 km to ERA5-Land resolution of about 9 km via a linear interpolation method based on a triangular mesh. Previous land reanalyses have included corrections to the precipitation forcing to address limitations of the precipitation fields of the atmospheric reanalysis. This is not the case in ERA5-Land (Muñoz-Sabater et al., 2021).

The core of ERA5-Land is the ECMWF land surface model: the Carbon Hydrology-Tiled ECMWF Scheme for Surface Exchanges over Land (CHTESSEL). The vegetation coverage in CHTESSEL corresponds to 2-dimensional static input fields. These fields provide, for each grid point, the fraction of low vegetation, the fraction of high vegetation, the dominant type of low vegetation, and the dominant type of high vegetation (Nogueira et al., 2020). A detailed description of the model can be found in Integrated Forecasting System (ECMWF, 2018)

Table 2. ERA5-LAND dataset description (Muñoz Sabater, 2019)

DATA DESCRIPTION	
Data type	Gridded
Projection	Regular latitude-longitude grid
Horizontal coverage	Global
Horizontal resolution	0.1° x 0.1°; Native resolution is 9 km
Vertical coverage	From 2 m above the surface level, to a soil depth of 289 cm.
Vertical resolution	4 levels of the ECMWF surface model: Layer 1: 0 -7cm, Layer 2: 7 -28cm, Layer 3: 28-100cm, Layer 4: 100-289cm Some parameters are defined at 2 m over the surface.
Temporal coverage	January 1950 to present
Temporal resolution	Hourly
File format	NetCDF
Update frequency	Monthly with a delay of about three months relatively to actual date

2.1.3 GLOBAL LAND DATA ASSIMILATION SYSTEM (GLDAS-2.0)

GLDAS, developed collaboratively by scientists from National Aeronautics and Space Administration (NASA), Goddard Space Flight Center (GSFC), and National Centers for Environmental Prediction (NCEP), aims to produce comprehensive fields related to land surface parameters (Rodell et al., 2004). The second version, GLDAS-2.0 (Table 3), replaced its previous data product on 19 November 2019 (Beaudoing and Rodell, 2019) and offers high-resolution data at 0.25 degrees. It provides 3-hourly, daily, monthly, and yearly mean values of precipitation (PT), Evapotranspiration (ET), and surface runoff (Q) (Voudouri et al., 2023). GLDAS-2.0 simulations are based on the Noah Model 3.6 and cover the period from January 1948 to December 2014, available in netCDF format (Beaudoing and Rodell, 2019). The data provided by GLDAS-2.0 is of high quality and covers various land surface fields on a global scale, making it valuable for climate and weather predictions, water cycle studies, and water resources applications (Voudouri et al., 2023)

Table 3. GLDAS-2.0 dataset description (Beaudoing and Rodell, 2019)

CONTENTS	OUTPUTS FROM LAND SURFACE MODELS
Format	NetCDF
Spatial Scale	Global
Longitude Extent	-180° to 180°
Spatial Resolution	0.25°
Temporal Resolution	3-hourly, daily, monthly
Temporal Coverage	GLDAS-2.0: 03Z January 1, 1948 – 21Z December 31, 2014
Dimensions	360 (lon) x 150 (lat) for the 1.0° x 1.0° data
	1440 (lon) x 600 (lat) for the 0.25° x 0.25° data
Origins (1st grid center)	(179.5 W, 59.5 S) for the 1.0° x 1.0° data
	(179.875 W, 59.875 S) for the 0.25° x 0.25° data
Land Surface Models	Noah-3.6, CLSM-F2.5, VIC-4.1.2

GLDAS_2.0 combines various land surface models, including Noah-3.6, CLSM-F2.5, and VIC-4.1.2. Each of these models has its own unique features and characteristics (Dai et al., 2003; Liang et al., 1994; Niu et al., 2011). In GLDAS_2.0, these models are coupled with data assimilation techniques to combine observational data with model outputs and improve the accuracy of the provided land surface variables. The combination of different models in

GLDAS allows researchers to analyze and compare outputs from multiple modeling approaches, aiding in a better understanding of global land surface processes and their interactions with the atmosphere (Beaudoing and Rodell, 2019; NASA , 2022).

In this study, we analyzed a long time series of data spanning from 1965 to 2014. The data comes from various models, namely CLM5, ERA5-Land, and GLDAS-2.0. The data was processed into monthly values for three key variables: PT, ET and Q.

2.2 METHOD

In this section, we describe the methodology used to calculate the GWR from the datasets. The GWR variables, namely evapotranspiration (ET), and surface runoff (Q), are direct outputs from the CLM5, ERA5-Land, and GLDAS datasets. To analyse and compare these datasets, we employed a comparative analysis approach, because it allows for the comparison of multiple models or datasets simultaneously. Python and R Studio have been used for the visualization of the results (maps and diagrams). As shown in Fig. 4, GWR was calculated using a water balance approach. The water balance approach (Eq.1) has the advantage of making use of pre-existing databases and satellite remote sensing data. Additionally, the upper soil layer's storage fluctuations can be ignored for long-term average calculations (Martinsen et al., 2022). For GWR calculation the unit of the variables was converted into millimetres per year (mm/year), the temporal resolution was divided into five decades, and we calculated the decadal mean of GWR based on yearly mean recharge within the decade. Subsequently, these means were plotted both continentally and regionally in the form of time series graphs (Eq.1).

$$GWR = PT - ET - Q \qquad (1)$$

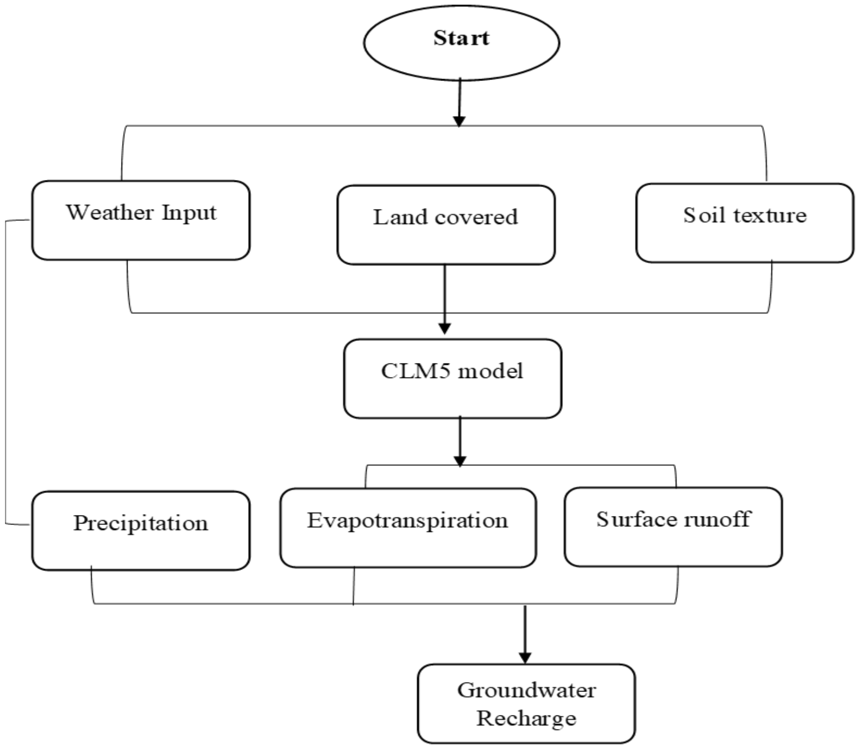

Figure 4. Adopted methodology in this study

2.2.1 STATISTICAL ANALYSIS

To evaluate the performance of the water balance analysis and examine the spatial and temporal relationships and agreements between the datasets, we utilized the following statistical measures: correlation coefficient (r), Root Mean Square Error (RMSE), and Kling-Gupta Efficiency (KGE). The correlation coefficient (r) (Eq.2) is used to quantify the strength and direction of the linear relationship between two variables. Its value ranges from -1 to +1, where ±1 indicates a perfect relationship, and 0 means there is no relationship between the observed and simulated values, ±0.9, ±0.8, ±0.7 meaning very strong relationship, ±0.6, ±0.5, ±0.4 meaning strong relationship, ±0.3 is moderate, ±0.2 is weak and ±0.1 is negligeable (Akoglu, 2018; Schober et al., 2018). RMSE measures the magnitude of errors in predictive models or estimation methods, helping assess accuracy and goodness of fit (Eq.3) (Chai and Draxler, 2014). KGE (Eq.4) is a comprehensive summary statistic considering the correlation, bias, and variability of a dataset (Wild et al., 2022). It provides a more holistic assessment of the model's performance compared to other metrics. KGE coefficient ranges from (-∞, 1], where a KGE value of 1 represents a perfect fit between observed and predicted values (Casati et al., 2023). We also make use of Taylor diagram to visualize the similarities and differences between multiple datasets in terms of their standard deviations, correlation coefficients, and root mean square difference.

$$r = \frac{\sum(X-\overline{X})(Y-\overline{Y})}{\sqrt{\sum(X-X)^2(Y-Y)^2}} \tag{2}$$

$$RMSE = \sqrt{\frac{1}{n}(X-Y)^2} \tag{3}$$

$$KGE = 1 - \sqrt{(r-1)^2 + (\beta-1)^2 + (\alpha-1)^2} \qquad \beta = \frac{\mu s}{\mu o} \qquad \alpha = \frac{\sigma s}{\sigma o} \tag{4}$$

Where: GWR is the Groundwater Recharge [mm/year], ET is the Evapotranspiration [mm/year], Q is the Surface Runoff [mm/year], r is the Pearson correlation coefficient, β is the bias term that is a ratio of the two datasets (e.g., CLM5 and ERA5) means and α is the variability term that is a ratio between the standard deviations of two dataset. X and Y are variables, $\overline{X}$ and $\overline{Y}$ denote the means of the two variables, n is the number of observations, X are observed measurements, Y simulated data.

2.2.2 TRIPLE COLLOCATION

Triple collocation analysis (TCA), which was first introduced by Stoffelen (1998), is an approach for estimating the error magnitude that compares geophysical products obtained using three or more independent estimation/observation techniques (Eq.5). Although it was initially created for ocean wind studies, the method is increasingly used in land surface hydrology (Yilmaz and Crow, 2014). TCA enables the estimation of error variances for three or more products (CLM5, ERA5-Land, and GLDAS) that retrieve or estimate the same geophysical variable using mutually independent methods (Yilmaz and Crow, 2014). TCA describes the simultaneous comparison of three datasets in this analysis (Eq.6). Although it is presumed that these datasets are independent of one another, they contain errors that result from a variety of sources, including instrumentation restrictions, data processing methods, or discrepancies in geographical and temporal sampling (Alemohammad et al., 2015).

$$\sigma^2_{ri} = C_{x,x} - \frac{Cx,y\ Cx,z}{Cy,z} \tag{5}$$

$$r_1 = \sqrt{\frac{C12\ C13}{C11\ C23}} \qquad r_2 = \sqrt{\frac{C12\ C23}{C22\ C13}} \qquad r_3 = \sqrt{\frac{C13\ C23}{C33\ C12}} \tag{6}$$

Where: σ_{ri} is the RMSE of the r_i product, **C** is the covariance matrix (3 x 3) of the datasets, the subscripts refer to the row and column numbers of the matrix and **r** is the correlation between each dataset. Perfect positive or negative agreement ($r = \pm1$), strong positive agreement ($0 < r < 1$), no linear correlation ($r = 0$) and strong Negative Agreement ($-1 < r < 0$). It should be noted that TCA analysis are generally based on statistical principles.

2.3 Study area

In this investigation, the delineation of distinct geographic regions within the study area (Fig.5) has been undertaken through a systematic partitioning process. The divisions are predicated on an analysis of climatic conditions and the homogeneity exhibited within each delineated region (Iturbide et al., 2020) .

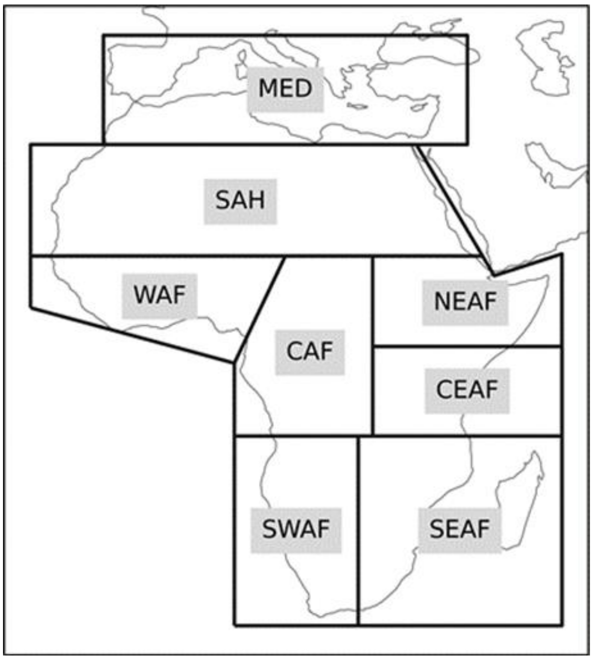

Figure 5. Map of regional division of Africa (Iturbide et al., 2020) where: MED is Mediterranean, SAH is Sahara, WAF is West Africa, CAF is Central Africa, NEAF is North-East Africa, CEAF is Central-East Africa, SWAF is South-West Africa and SEAF is South-East Africa)

PARTIAL CONCLUSION

The dataset processing procedures and methodological approaches employed herein have facilitated the derivation of results, which are expounded upon in the subsequent chapter. In circumstances characterized by constraints in acquiring in situ measurements, the application of models and reanalysis datasets through comparative methodologies assumes a pivotal role. Specifically, these methodologies serve as instrumental tools in elucidating the intricate spatiotemporal patterns governing Groundwater Recharge (GWR) across the African continent.

Chapter 3: RESULTS and DISCUSSION

Chapter 3: RESULTS and DISCUSSION

INTRODUCTION

In this chapter, we systematically present and rigorously analyse the outcomes of our study. Our analytical approach encompasses a comprehensive discussion that draws upon existing literature for comparative insights. Notably, our focus is directed towards specific African regions, as illustrated in Figure 5, which have been selected as key areas of interest. Our analytical journey commences with an in-depth exploration of the PT, ET, and Q patterns. This initial analysis forms the foundational understanding for the assessment of Groundwater Recharge (GWR). Furthermore, the results of statistical metrics are meticulously presented, affording a clear perspective on the accuracy and interrelationships inherent to the employed models. Beyond elucidating the hydrological aspects, we delve into the implications of GWR within the context of green hydrogen production. Additionally, we critically evaluate the inherent limitations of our approach, thus offering a holistic perspective on the findings and their potential ramifications.

3.1 RESULTS and DISCUSSION

3.1.1 Precipitation pattern

Fig. 6 presents the spatiotemporal distribution of mean decadal precipitation across Africa from 1965 to 2014, as estimated by three different models (ERA5-Land, and GLDAS-2.0). Across the continent, there is a notable similarity in the precipitation patterns among the models. Regions such as Central Africa (CAF), Central-East Africa (CEAF), West Africa (WAF), South-East Africa (SEAF), and North-East Africa (NEAF) (including Ethiopia) receive higher levels of precipitation, ranging from 556 to 1000 mm/year. Notably, countries like the Democratic Republic of the Congo, Angola, Cameroon, Equatorial Guinea, and Gabon experience particularly high levels of precipitation. In West Africa (WAF), countries such as Guinea, Liberia, Sierra Leone, Côte d'Ivoire, Nigeria, Togo, Benin, and Guinea-Bissau also receive comparatively higher precipitation compared to other WAF countries. In contrast, the Sahara (SAH), Mediterranean (MED), South-West Africa (SWAF), and NEAF received less precipitation, ranging from 100 to 556 mm/year, with SAH and MED exhibiting the lowest precipitation levels. Examining the temporal variation, ERA5-Land recorded the highest mean precipitation values, ranging from 643.1 to 727.3 mm/year over the five decades, followed by CLM5, with values varying from 643.2 to 656.2 mm/year as averages over the five decades. GLDAS_2.0 had the lowest precipitation mean values, ranging from 610.4 to 642.9 mm/year.

Over the decades, CLM5 and GLDAS showed a decrease in mean precipitation values during the first three decades, followed by an increase in the last two decades. Conversely, ERA5-Land demonstrated an increase in mean precipitation during the first decade but consistently decreased in the following decades.

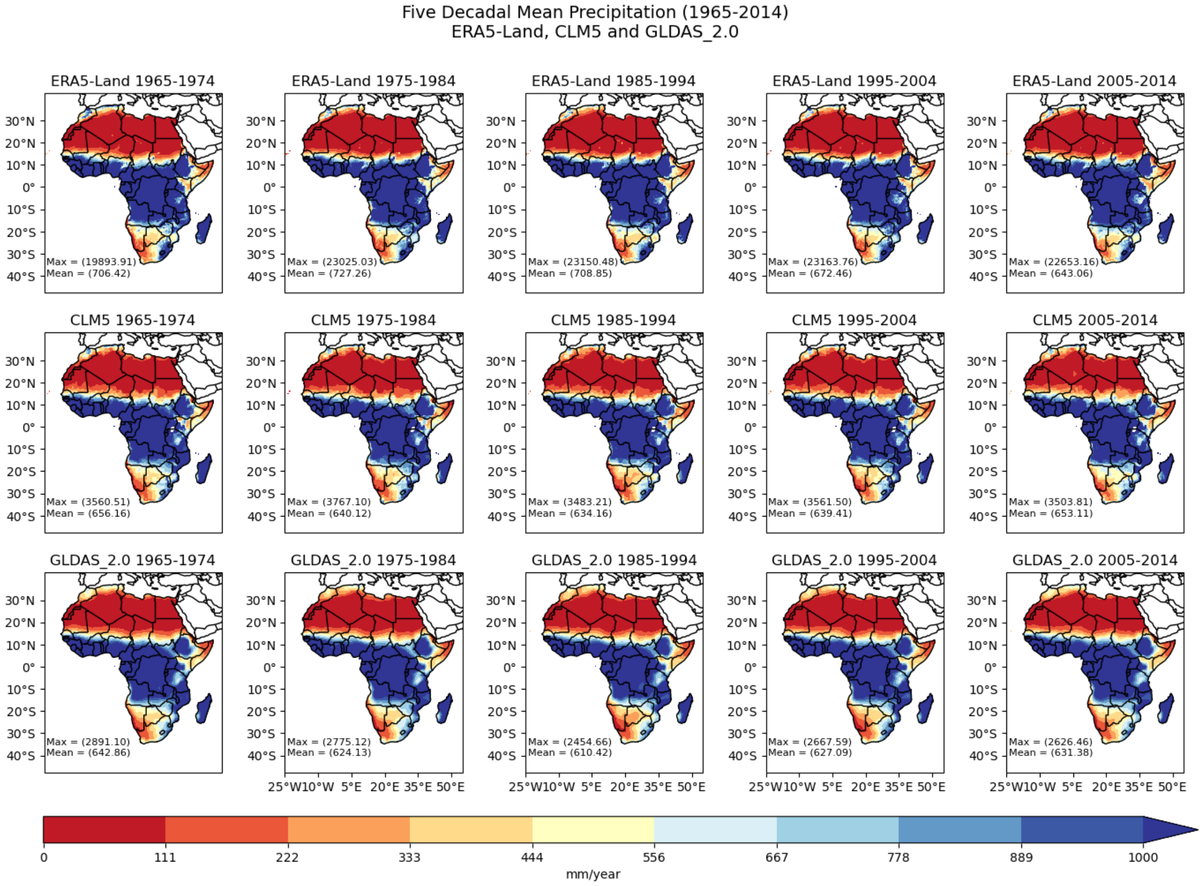

Figure 6. The decadal mean precipitation patterns in Africa from 1965 to 2014, representing three distinct datasets. The top row shows ERA5-Land, the middle row shows CLM5 and the bottom row shows GLDAS_2.0. The figures are arranged from left to right, representing the first to the fifth decade, respectively.

3.1.2 Evapotranspiration Pattern

Fig. 7 displays the spatiotemporal distribution of Evapotranspiration (ET) across the African continent. There is a strong correlation between ET and the precipitation pattern for all the models. Regions with higher precipitation levels, such as CAF, CEAF, WAF, SWAF, and NEAF, also experienced higher ET values ranging from 444 to 1000 mm/year. In terms of temporal variation, CLM5 and GLDAS_2.0 showed a decrease in ET mean values during the first three decades, followed by an increase in the last two decades. However, ERA5-Land did not exhibit a clear pattern in its temporal variation. Conversely, regions with lower precipitation levels, like MED, SAH, SWAF, and NEAF, had lower ET values ranging from 111 to 556 mm/year. Analysing the temporal variation, ERA5-Land recorded the highest ET mean values, ranging from 517 to 539.4 mm/year, followed by CLM5 with ET mean values ranging from 471.4 to 487.4 mm/year. GLDAS had the lowest ET mean values, ranging from 454.4 to 470.3 mm/year.

This study compared three models (CLM5, ERA5-Land, and GLDAS) in terms of PT and ET at both continental and regional scales. It is found that regions like CAF, CEAF, WAF, SEAF, and NEAF (including Ethiopia) received higher levels of PT and ET, ranging from 556 to 1000 mm/year and 444 to 1000 mm/year, respectively (Fig. 6 & 7). In contrast, SAH, MED, and SWAF received lower amounts. These findings are consistent with previous studies by (Dieulin et al., 2019; MacDonald and Calow, 2009; Weerasinghe et al., 2020) which also reported similar spatial and temporal patterns of PT and ET. However, it's important to note that the mean values of PT and ET varied among different studies, as in this study decadal means have been presented.

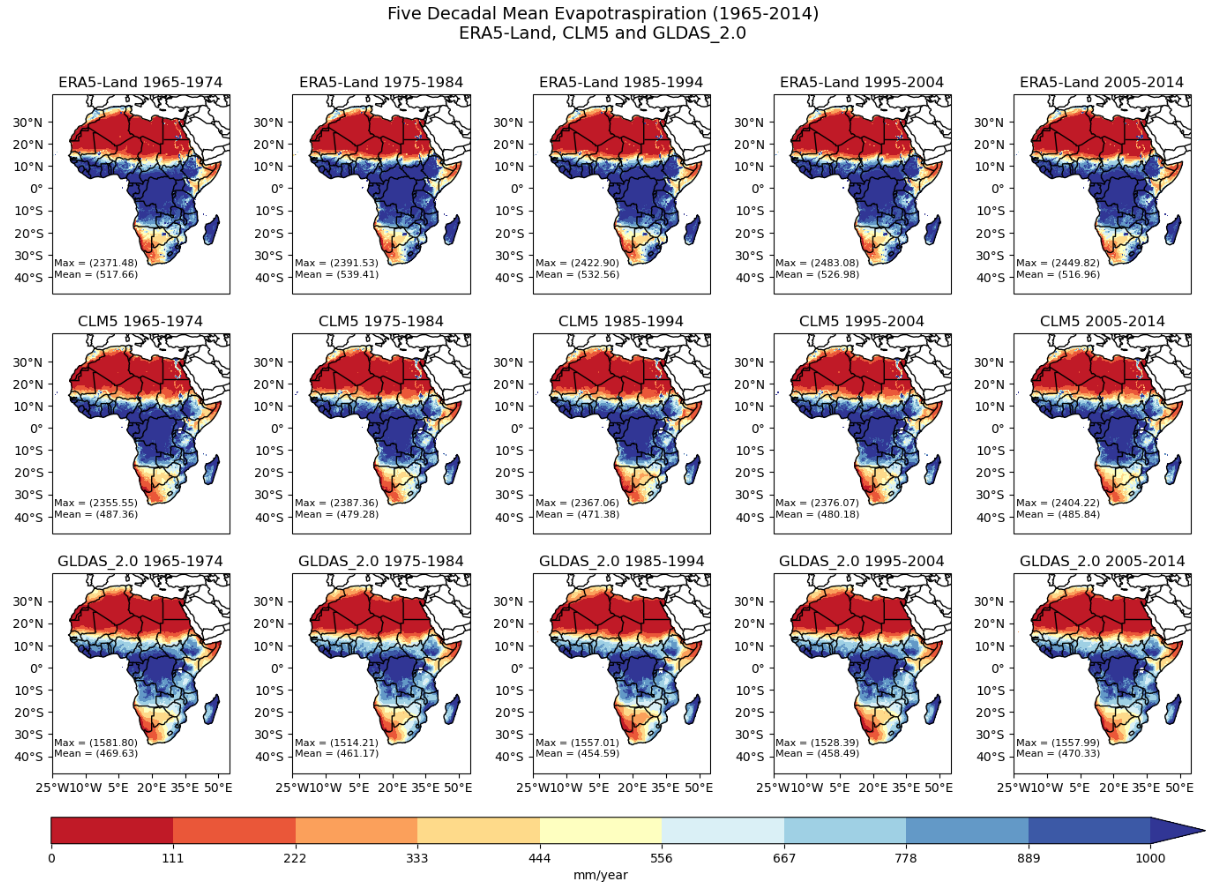

Figure 7. Decadal mean evapotranspiration patterns in Africa from 1965 to 2014, representing three distinct datasets. The top panel shows ERA5-Land, the middle panel shows CLM5 and the bottom panel shows GLDAS_2.0. The figures are arranged from left to right, representing the first to the fifth decade, respectively.

3.1.3 Surface Runoff

The spatiotemporal distribution of Surface Runoff (Q) in Fig. 8 varies significantly among the different models. ERA5-Land and CLM5 exhibit the highest Q values in regions like CAF, WAF, CEAF, NEAF, and SEAF. Analysing the temporal variation, CLM5 records the highest Q mean values, ranging from 122.8 to 128.0 mm/year, with a notable impact in countries like Guinea, Liberia, Sierra Leone, Nigeria, Cameroon, Equatorial Guinea, and Madagascar. On the other hand, ERA5-Land records moderate Q mean values, ranging from 48.1 to 56.8 mm/year. Conversely, GLDAS_2.0 displays the lowest Q mean values (10.0 to 10.8 mm/year) across the entire continent, with some regions like CAF, CEAF, and NEAF showing only a small difference compare to other regions. Overall, the Q patterns differ substantially among the models, with CLM5 and ERA5-Land showing higher values in specific regions, while GLDAS_2.0 consistently presents lower Q values across the entire African continent.

One significant difference between the models was observed in the calculation of Q, the overall decadal mean of CLM5 is 124.38 mm/year, ERA5-Land is 53.52 mm/year while for GLDAS_2.0 is 10.52 mm/year. Land use/land cover and Q parameterization have been examined and it is found that, CLM5 used the simple TOPMODEL-based runoff model (SIMTOP), which represents the discrete distribution of the topographic index as an exponential function (Niu et al., 2005), the present-day global land cover descriptions are generated at 1-km resolution (Lawrence et al., 2019), in SIMTOP precipitation that falls over the saturated fraction of a grid cell is immediately converted to Q. Surface runoff at the study site is almost absent (Denager et al., 2023). In contrast, ERA5-Land uses a hydrological model based on the HTESSEL land surface which is a revised land surface Hydrology Tiled ECMWF Scheme for Surface exchanges over land (Balsamo et al., 2009). For the standard formulation of ERA5, land cover, and vegetation, the Carbon Hydrology Tiled (CHTESSEL) Scheme has been used for Surface Exchanges over Land (Nogueira et al., 2021), which does not benefit from the development of vegetation data sets during the past 20 years. In the case of Q, it has been calculated as a sum of throughfall PT, the snow melting (M) subtracted by the maximum infiltration rate, I_{max} (ECMWF, 2018). While GLDAS2.0 estimated runoff based on global land surface models (LSMs) and forcing data from the Princeton Global Meteorological Forcing (PGF) dataset (Qi et al., 2020). These differences in Q calculation and land use/land cover representations within the models likely contribute to the varying Q values among them. Notably, previous studies have highlighted uncertainties in GLDAS2.0 data. Wang et al. (2016), assessed the soil temperature estimation of GLDAS2.0 and found good agreement with in situ measurement studied the applicability of GLDAS2.0 in terms of PT, ET, air temperature, water storage, and runoff and they found that runoff is underestimated. Qi et al. (2020), compares uncertainties in runoff estimations of GLDAS versions 2.0 and 2.1 in China and found large uncertainties in Q, for instance, absolute values of relative bias (|RB|) being above 39% and Nash-Sutcliffe efficiency lower than 0.15 on average, furthermore, concluded that GLDAS2.1 is better than GLDAS2.0. Q values found in this study give evidence of uncertainty in Q for GLDAS2.0 that has been highlighted in the previous studies.

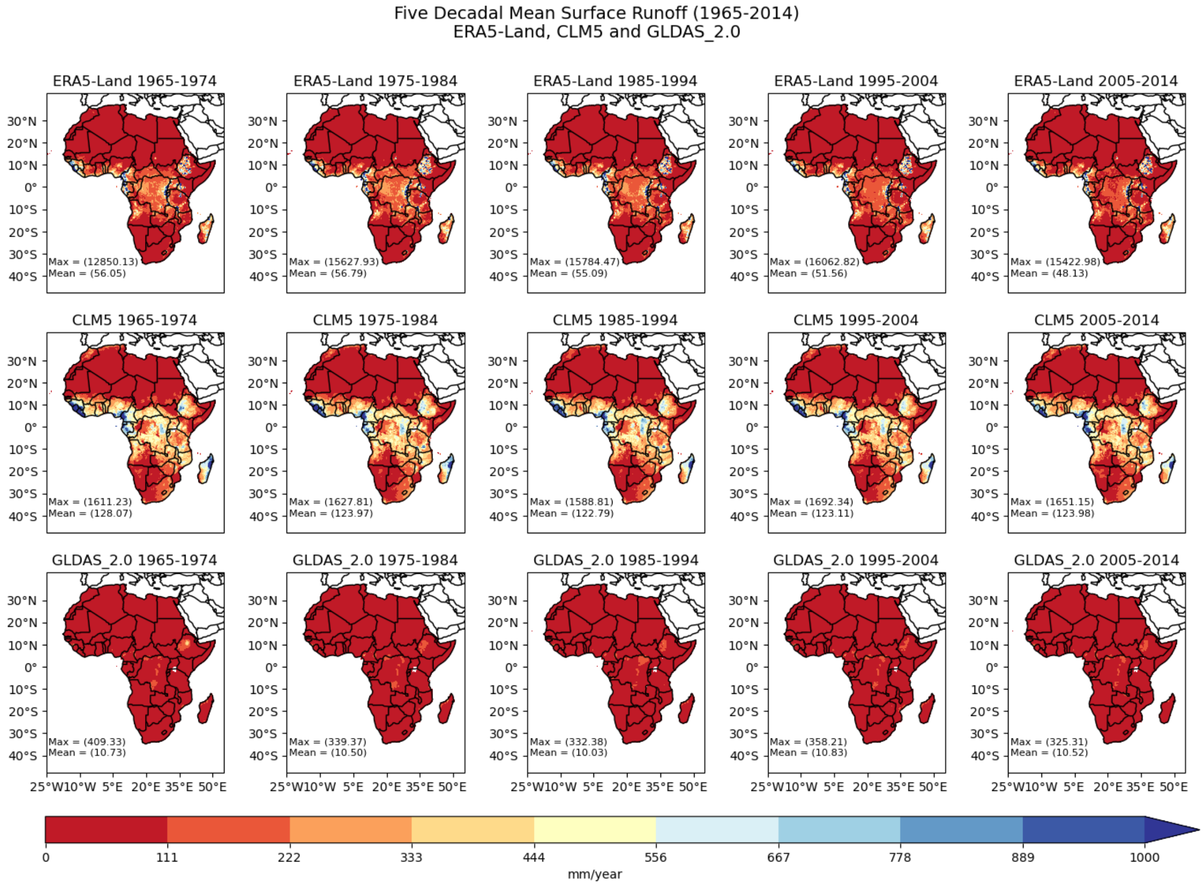

Figure 8. Decadal mean surface runoff patterns in Africa from 1965 to 2014, representing three distinct datasets. The top panel shows ERA5-Land, the middle panel shows CLM5 and the bottom panel shows GLDAS_2.0. The figures are arranged from left to right, representing the first to the fifth decade, respectively.

3.1.4 Comparative Time Series Analysis of PT, ET, and Q in African Regions

In this section, our focus is on investigating the temporal dynamics of PT, ET, and Q within different African regions using all three models (CLM5, ERA5-Land, and GLDAS) as depicted in Figures 9 and 10. Our analysis uncovers intriguing trends and patterns in these variables across the regions. When examining PT and ET in the MED, SAH, WAF, and SEAF regions, we find consistent temporal trends across all three models. However, variations in magnitude are evident, with ERA5-Land displaying notably higher values in WAF and SEAF. The MED and SAH regions exhibit a remarkable harmony in both trends and magnitudes, maintaining relatively stable patterns, ranging from 200 to 300 mm/year for both PT and ET. Notably, SAH stands out as an exceptionally stable region, with PT and ET differing by approximately 110 mm/year. Contrasting this, Q exhibits distinctive trends and magnitudes, particularly pronounced in WAF and SEAF. In terms of the models' performance, CLM5 records the highest Q values, trailed by ERA5-Land, while GLDAS presents the lowest values for these regions. On the other hand, NEAF, CEAF, SWAF, and CAF regions showcase distinct temporal variability in trends and magnitudes. In PT, CAF and CEAF stand out with higher temporal variability compared to NEAF and SWAF. Yet, when it comes to ET, these regions exhibit comparable trends. Across the board, ERA5-Land consistently demonstrates the highest magnitudes for both PT and ET, prominently seen in CAF and CEAF (PT ≈ 1700 mm/year and ET ≈ 1000 mm/year). The comparative analysis reveals marked disparities in Q among all regions. CLM5 registers notably elevated Q values in WAF, CAF, SEAF, NEAF, and CEAF, ranging from 130 to 300 mm/year. In contrast, MED and SAH exhibit the lowest Q levels.

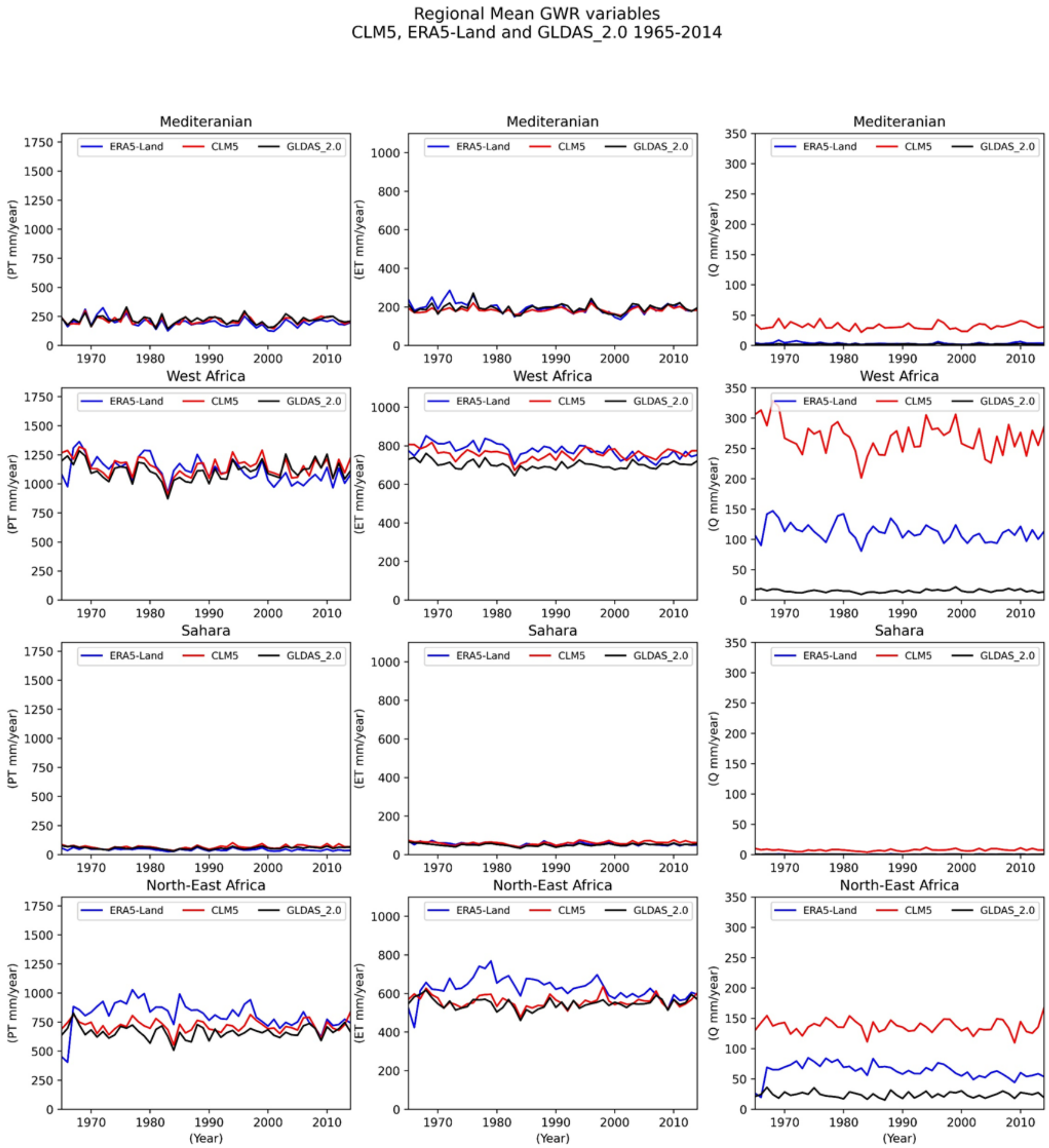

Figure 9. Comparative analysis of temporal variation in Precipitation (PT), Evapotranspiration (ET), and Surface Runoff (Q) across African regions using CLM5, ERA5-Land, and GLDAS datasets. PT is represented on the left, ET in the middle, and Q on the right.

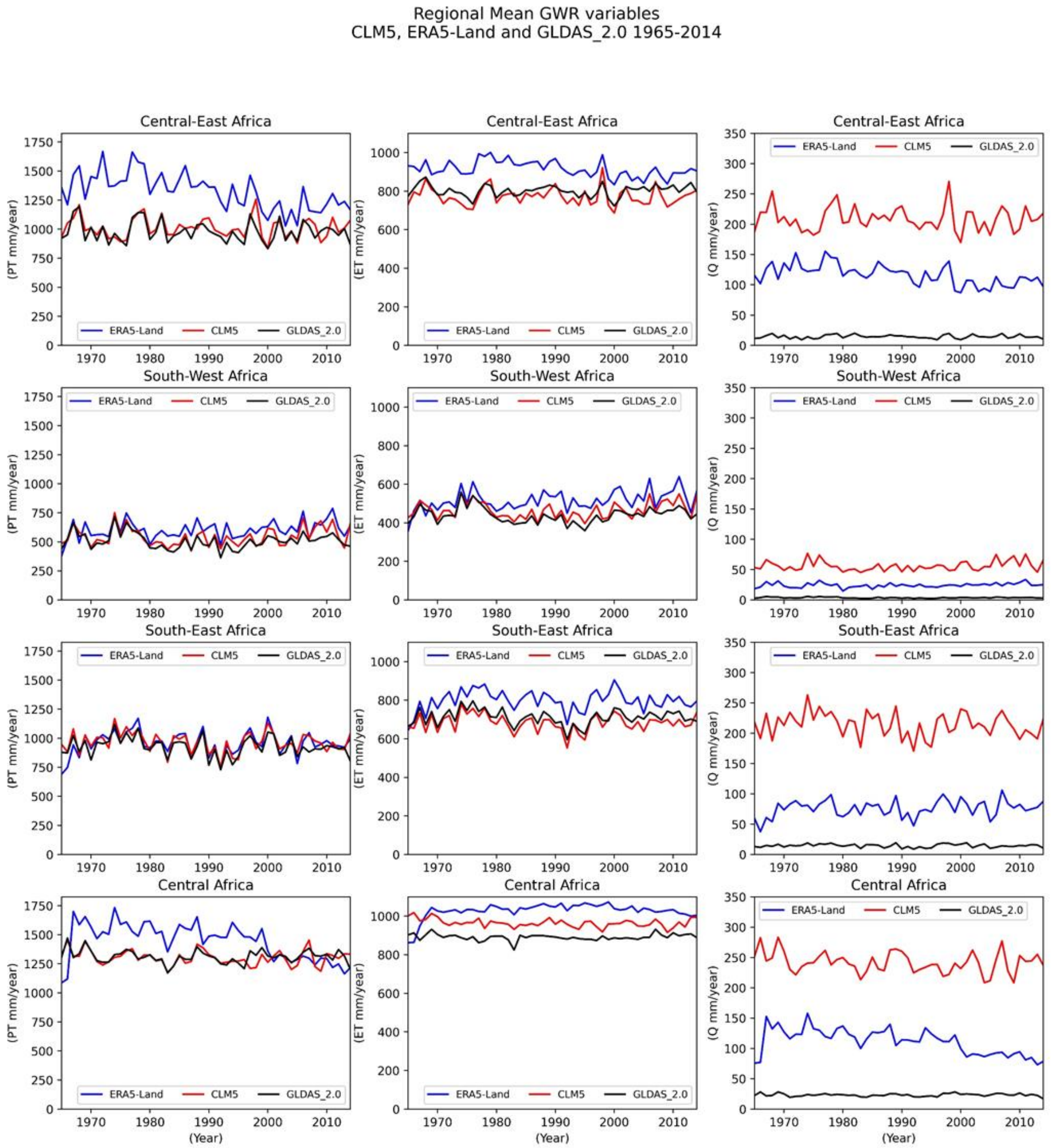

Figure 10. Comparative Analysis of Temporal Variation in Precipitation (PT), Evapotranspiration (ET), and Surface Runoff (Q) across African Regions using CLM5, ERA5-Land, and GLDAS Datasets. PT is represented on the left, ET in the middle, and Q on the right.

3.1.5 Comparative Analysis of Spatial Distribution of GWR

In this section, we analyse the spatial distribution of GWR for five decades (Fig. 11). Our findings reveal that ERA5-Land and GLDAS consistently show higher GWR than CLM5 in specific regions, including CAF, WAF, CEAF, NEAF (specifically Ethiopia), and SEAF (specifically Madagascar). In WAF, countries such as Guinea-Bissau, Guinea, Liberia, Sierra Leone, and the northern part of Nigeria exhibit the highest GWR (667 – 1000 mm/year). Similarly in CAF, Gabon, Equatorial Guinea, Cameroon, and the Democratic Republic of Congo receive substantial GWR over time. Notably, GWR availability appears more pronounced in the mentioned regions for ERA5-Land compared to GLDAS, ranging from 111 to 1000 mm/year over the study period. In contrast, CLM5 shows comparatively lower GWR availability in CAF, WAF, CEAF, NEAF, and SEAF compared to ERA5-Land and GLDAS_2.0. Only a few countries in CLM5, such as Guinea-Bissau, Guinea, Liberia, Sierra Leone, the northern part of Nigeria, and the Democratic Republic of Congo, show higher GWR availability than for the other two models. Comparing the mean GWR over time, GLDAS records the highest values (147.8 to 164.1 mm/year), followed by ERA5-Land (96.1 to 151.8 mm/year), while CLM5 shows the lowest GWR values over the study period (42.3 to 48.5 mm/year). Additionally, the models show agreement in regions with lower GWR availability, such as MED, SAH, NEAF, SWAF, and the southern part of Madagascar, where GWR is recorded as ranging from 0 to 222 mm/year.

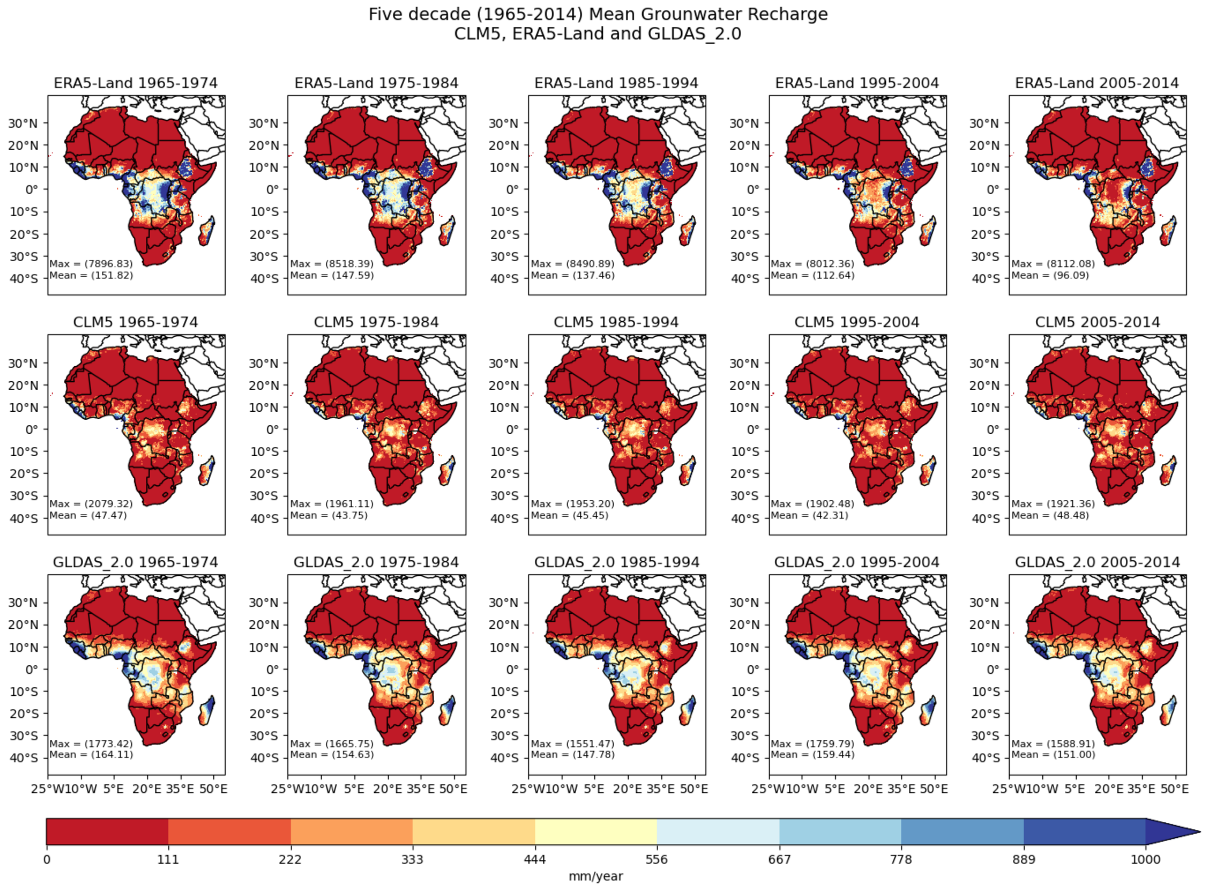

Figure 11. Decadal mean groundwater recharge spatial distribution in Africa from 1965 to 2014, representing three distinct datasets. The top panel shows ERA5-Land, the middle panel shows CLM5 and the bottom panel shows GLDAS_2.0. The figures are arranged from left to right, representing the first to the fifth decade, respectively.

3.1.6 Comparative Time Series Analysis of Groundwater Recharge (GWR)

In this section, we examine the temporal variation of GWR across African regions (Fig. 12). The results indicate that WAF, CAF, CEAF, and SEAF experienced higher GWR levels ranging from 25 to 600 mm/year during the study period. While WAF, SAH, and SWAF display similar trends, there are differences in magnitude. In regions such as MED, WAF, SAH, and SEAF, GLDAS records the highest GWR values, followed by ERA5-Land. However, in CEAF and NEAF, ERA5-Land shows the highest GWR values. Conversely, MED, SAH, and SWAF exhibit the lowest GWR values across the continent, ranging from 0 to 150 mm/year. The highest peak in GWR is recorded in the first decade in CAF and CEAF, reaching 600 and 580 mm/year, respectively. Significant differences in trends between the models are observed in CAF, SEAF, and CEAF over time. It is evident that CLM5 consistently records the lowest GWR values compared to ERA5-Land and GLDAS in all regions. The simulated GWR values of ERA5-Land and GLDAS are closer to each other than the ones of CLM5. Notably, ERA5-Land exhibits a decrease in magnitude over time in CAF, WAF, NEAF, and particularly in

CEAF. This time series analysis provides valuable insights into the spatiotemporal variability of GWR and the performance of the three models across African regions, facilitating a deeper understanding of groundwater recharge dynamics in the continent.

Using a water budget approach, a comparative analysis was conducted to assess the spatiotemporal distribution of GWR among three models: ERA5-Land, GLDAS_2.0, and CLM5. The results showed that regions like CAF, CEAF, WAF, NEAF, and SEAF had high GWR availability, while SAH, MED, and SWAF exhibited lower availability. Interestingly, CLM5 showed comparatively lower GWR availability in CAF, WAF, CEAF, NEAF, and SEAF compared to ERA5-Land and GLDAS_2.0. The overall decadal mean of GWR for ERA5-Land was 129.92 mm/year and for GLDAS_2.0 was 155.39 mm/year. These findings were in line with previous studies, including Mileham et al. (2008), Adeleke et al. (2015), and Abiye (2016), who reported mean annual recharge values ranging from 104 to 194.7 mm/year in various regions. On the other hand, CLM5 presented a lower overall decadal mean of 45.49 mm/year, largely influenced by the high Q reported in the model. Interestingly, some studies have reported results similar to CLM5. For example, (Sibanda et al., 2009) compared various GWR estimation methods in Zimbabwe and found values ranging from 11 to 250 mm/year. (Xu and Beekman, 2019) assessed GWR estimation in southern Africa and reported recharge values of 10 to 50 mm/year. Wang et al. (2010) reviewed recharge estimation and groundwater resource assessment in Africa and reported initial estimates of regional recharge ranging from 50 to 60 mm/year in the Sahel region. Overall, the findings of this study align with previous research and provide valuable insights into GWR comparison using different models.

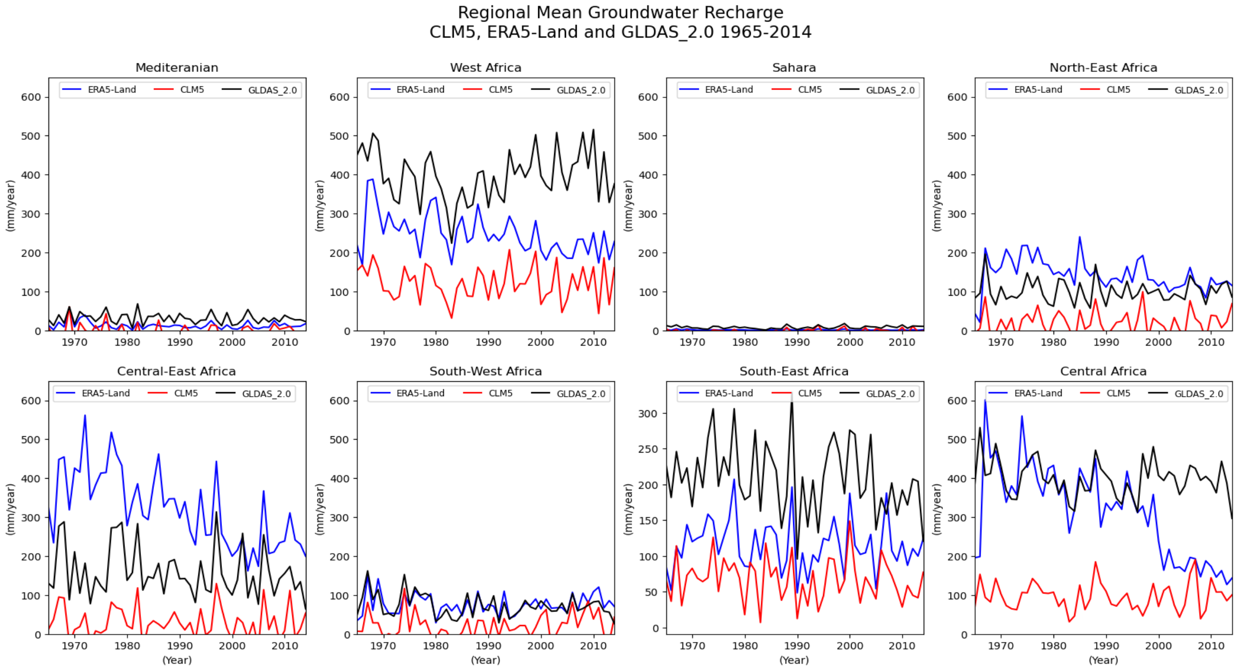

Figure 12. Comparative analysis of temporal variation in mean groundwater recharge across African regions for the period covering 1965 - 2014 using CLM5, ERA5-Land, and GLDAS Datasets.

3.1.7 Error metrics

3.1.7.1 Presentation of results

In this section, we have conducted an extensive analysis of statistical error metrics using a variety of methodologies. The outcomes of this analysis, which encompass a wide range of groundwater balance components for each region, are meticulously presented in Table 4. Our primary objective is to perform a comparative evaluation of ERA5-Land and GLDAS_2.0 against the reference model, CLM5, within specified regions. Additionally, we have consistently applied a specific methodology to compute error metrics for Groundwater Recharge (GWR) across each region, as elaborated in Table 5. To enhance the rigor and comprehensiveness of our analysis, we have harnessed the power of Triple Collocation Analysis (TCA), as exemplified in Table 6. This approach allows us to delve into the intricate interactions among the three datasets - CLM5, ERA5-Land, and GLDAS_2.0. Moreover, we have employed a visual tool, the Taylor diagram (Figure 13), to assess the performance of each model in comparison to the reference model. This diagram provides a concise representation of key metrics such as the correlation coefficient, standard deviation, and root mean square distance, all presented in a single plot for clarity and ease of interpretation.

Table 4 presents the r, RMSE, and KGE values for different regions, models, and variables in the study. The variables of ERA5-Land and GLDAS were analysed and compared with the reference model CLM5 in specific regions. The results indicated positive correlations between the variables in almost all regions, except for CAF, where CLM5 and ERA5-Land exhibited a negative correlation (-0.42) for ET. PT showed good to very good correlations (0.4 to 0.9) in most regions, except for NEAF and CAF, where CLM5 and ERA5-Land showed values of 0.28 and 0.39, respectively. Q had correlation values ranging from 0.07 to 0.86, and ET had values ranging from -0.42 to 0.92. Considering all variables, the RMSE values ranged from 7.2 to 313.5 mm/year, SAH and MED had the lowest RMSE, while WAF, NEAF, CEAF, SEAF, and CAF had the highest RMSE for Q. The lowest RMSE (7.2 mm/year) was recorded for PT in SEAF, while the highest RMSE (313.5 mm/year) was recorded for PT in CEAF. Notably, Q had the highest RMSE values among the variables. Positive KGE agreement was found for PT and ET in almost all regions, except for CAF. However, for Q, all models and regions displayed negative KGE values (-0.13 to -24.9). Comparison between CLM5 and GLDAS showed a very good correlation, with RMSE values in all regions greater than ERA5-Land for Q. Additionally, there was a good agreement between CLM5 and GLDAS for PT and ET, with KGE values between CLM5 and GLDAS indicating good to very good agreement compared to ERA5-Land. Regarding Q, CLM5, and ERA5-Land showed a closer relationship compared to GLDAS. Overall, the Table 4 provides valuable insights into the performance and agreement of the models for different variables and regions, contributing to a comprehensive understanding of the study's findings.

Table 4. Comparative Analysis of Correlation Coefficient, RMSE, and KGE Values for Precipitation, Evapotranspiration, and Surface Runoff in different African regions.

Regions	Variables	Models	r	RMSE	KGE
Mediterranean	Precipitation	CLM5 & ERA5	0.800	13.048	0.750
		CLM5 & GLDAS_2.0	0.893	8.554	0.877
	Evapotranspiration	CLM5 & ERA5	0.762	12.971	0.422
		CLM5 & GLDAS_2.0	0.9245	10.193	0.592
	Surface Runoff	CLM5 & ERA5	0.776	28.236	-7.196
		CLM5 & GLDAS_2.0	0.857	29.882	-16.324
West Africa	Precipitation	CLM5 & ERA5	0.579	31.358	0.554
		CLM5 & GLDAS_2.0	0.911	34.992	0.899
	Evapotranspiration	CLM5 & ERA5	0.45	16.237	0.4102
		CLM5 & GLDAS_2.0	0.725	56.61	0.579
	Surface Runoff	CLM5 & ERA5	0.576	155.78	-0.655
		CLM5 & GLDAS_2.0	0.795	253.286	-18.636
Sahara	Precipitation	CLM5 & ERA5	0.618	23.625	0.167
		CLM5 & GLDAS_2.0	0.871	9.644	0.515
	Evapotranspiration	CLM5 & ERA5	0.555	5.385	0.542
		CLM5 & GLDAS_2.0	0.875	10.083	0.619
	Surface Runoff	CLM5 & ERA5	0.532	6.981	-12.16
		CLM5 & GLDAS_2.0	0.764	7.234	-24.914
North-East Africa	Precipitation	CLM5 & ERA5	0.277	91.338	0.091
		CLM5 & GLDAS_2.0	0.755	52.38	0.743
	Evapotranspiration	CLM5 & ERA5	0.144	65.825	0.011
		CLM5 & GLDAS_2.0	0.794	12.004	0.788
	Surface Runoff	CLM5 & ERA5	0.253	73.267	-0.383
		CLM5 & GLDAS_2.0	0.374	112.796	-3.917
Central-East Africa	Precipitation	CLM5 & ERA5	0.462	313.473	0.274
		CLM5 & GLDAS_2.0	0.734	33.111	0.731
	Evapotranspiration	CLM5 & ERA5	0.645	142.164	0.596
		CLM5 & GLDAS_2.0	0.702	29.164	0.402
	Surface Runoff	CLM5 & ERA5	0.489	92.43	0.040
		CLM5 & GLDAS_2.0	0.688	194.323	-13.609
South-West Africa	Precipitation	CLM5 & ERA5	0.741	59.422	0.723
		CLM5 & GLDAS_2.0	0.808	35.355	0.741
	Evapotranspiration	CLM5 & ERA5	0.722	50.761	0.661
		CLM5 & GLDAS_2.0	0.854	25.653	0.82
	Surface Runoff	CLM5 & ERA5	0.633	31.877	-0.851
		CLM5 & GLDAS_2.0	0.651	52.446	-15.601
South-East Africa	Precipitation	CLM5 & ERA5	0.774	7.208	0.736
		CLM5 & GLDAS_2.0	0.812	38.626	0.804
	Evapotranspiration	CLM5 & ERA5	0.81	114.194	0.711
		CLM5 & GLDAS_2.0	0.907	26.588	0.862
	Surface Runoff	CLM5 & ERA5	0.629	138.296	-0.915
		CLM5 & GLDAS_2.0	0.701	199.752	-14.146
Central Africa	Precipitation	CLM5 & ERA5	0.039	139.719	-0.132
		CLM5 & GLDAS_2.0	0.68	8.515	0.651
	Evapotranspiration	CLM5 & ERA5	-0.421	63.599	-0.494
		CLM5 & GLDAS_2.0	0.392	73.318	0.309
	Surface Runoff	CLM5 & ERA5	0.073	130.501	-0.505
		CLM5 & GLDAS_2.0	0.542	218.655	-10.394

3.1.7.2 Assessment Groundwater Recharge Models

In this section, we present the r, RMSE, and KGE values for GWR in different regions and models studied. We analysed GWR data from ERA5-Land and GLDAS, comparing them with the reference model CLM5 in specific regions (Table 5). The results demonstrate a positive correlation between the models in all regions, ranging from 0.118 to 0.816. SAH, MED, SEAF, and SWAF exhibit the highest correlation values for both models, while CAF shows the lowest correlation between CLM5 and ERA5-Land (0.118). In general, the correlation between CLM5 and GLDAS is higher compared to that between CLM5 and ERA5-Land. Across all regions, the correlation varies from good to very good, except for CAF. When comparing CLM5 with GLDAS, the lowest RMSE values are generally observed, except in SEAF where the RMSE for CLM5 & GLDAS is 38.5 mm/yr and for CLM5 & ERA5-Land 27.6 mm/yr. In terms of KGE, a negative KGE is observed in almost all regions, indicating poor agreement between the models and the reference data (CLM5). However, the comparison between CLM5 and GLDAS reveals a positive KGE in NEAF and SWAF (0.415 and 0.458), while for CLM5 and ERA5-Land it is positive for SEAF (0.139). MED and SAH regions show the poorest agreement (KGE of -3.178 and -3.377), while NEAF stands out as the region with more acceptable KGE values (0.139 and -0.295). These findings provide valuable insights into the performance and agreement of the models for GWR in different regions, guiding the understanding of groundwater recharge dynamics and identifying regions with potential for model improvement.

The statistical analysis and time series (Tables 4 and 5, Fig. 9 & 10) showed that CLM5 exhibited a stronger correlation with GLDAS_2.0 than with ERA5-Land. Due to the low moisture content, regions such as SAH, MED, and SWAF demonstrated better model performance with higher correlation, lower RMSE, KGE scores. On the other hand, CAF, CEAF, and NEAF exhibited the highest moisture content hence, the worst model performance. Regions such as SAH, MED, SEAF, and SWAF showed better model performance, while CAF, CEAF, WAF, and NEAF exhibited less satisfactory results.

Table 5. Comparative Analysis of Correlation Coefficient, RMSE, and KGE Values for Groundwater Recharge (GWR) in Different Regions and Models (CLM5, ERA5-Land, and GLDAS)

Regions	Models	r	RMSE	KGE
Mediterranean	CLM5 & ERA5	0.662	15.233	-3.178
	CLM5 & GLDAS_2.0	0.723	13.753	-3.377
West Africa	CLM5 & ERA5	0.506	47.638	-0.2105
	CLM5 & GLDAS_2.0	0.816	37.782	-0.878
Sahara	CLM5 & ERA5	0.695	5.12	-1.094
	CLM5 & GLDAS_2.0	0.778	3.721	-2.206
North-East Africa	CLM5 & ERA5	0.454	38.719	-5.188
	CLM5 & GLDAS_2.0	0.733	21.447	0.415
Central-East Africa	CLM5 & ERA5	0.471	84.338	-8.679
	CLM5 & GLDAS_2.0	0.767	42.653	-0.202
South-West Africa	CLM5 & ERA5	0.583	26.865	-1.597
	CLM5 & GLDAS_2.0	0.685	24.196	0.458
South-East Africa	CLM5 & ERA5	0.653	27.55	0.139
	CLM5 & GLDAS_2.0	0.639	38.468	-0.295
Central Africa	CLM5 & ERA5	0.118	117.629	-1.785
	CLM5 & GLDAS_2.0	0.618	37.564	-0.815

3.2.7.3 Triple Collocation Analysis

Table 6 shows the results of the triple collocation analysis (TCA) between the three datasets (CLM5, ERA5, and GLDAS). RMSE (R1, R2, R3) and correlation coefficients (cor1, cor2, cor3) have been calculated for each dataset compared to the others using Eq. 5 & 6. The results reveal a positive correlation for each dataset across all regions, with correlation coefficients ranging from good to excellent (0.48 to 1.0). Specifically, regions such as MED, SAH, and SWAF demonstrate higher correlation for all datasets, while WAF, CEAF, and CAF exhibit comparatively lower correlation values. Notably, WAF (cor1) and CEAF (cor3) show excellent correlation levels. Regarding RMSE, all individual datasets present values ranging from 0.614 to 115.49, CAF shows the highest RMSE value, where R2 is 115.49. At the regional level, SAH, MED, and SEAF exhibit the lowest RMSE, indicating better overall performance of the models in these regions. Conversely, CAF, CEAF, and WAF show the highest RMSE values, suggesting relatively lower model performance in these regions. The findings underscore that the models perform better in regions such as SAH, MED, and SEAF, where the correlation is higher and RMSE values are lower. However, CAF and WAF regions present challenges, with lower correlation and higher RMSE values, indicating areas where model improvements may be beneficial.

Table 6. Comparing Geophysical Variable Measurements using Triple Collocation Method: Assessing Correlation and RMSE across different regions and datasets

Regions	RMSE		Cor coef.	
Mediterranean	R1	11.58	cor1	0.817
	R2	5.99	cor2	0.81
	R2	6.538	cor3	0.88
West Africa	R1	27.92	cor1	1.0
	R2	45.31	cor2	0.48
	R3	39.85	cor3	0.785
Sahara	R1	3.093	cor1	0.85
	R2	0.614	cor2	0.82
	R3	1.501	cor3	0.91
North-East Africa	R1	12.56	cor1	0.91
	R2	36.34	cor2	0.49
	R3	16.88	cor3	0.8
Central-East Africa	R1	26.28	cor1	0.76
	R2	75.81	cor2	0.62
	R3	57.76	cor3	1.0
South-West Africa	R1	19.59	cor1	0.77
	R2	18.59	cor2	0.85
	R3	27.94	cor3	0.83
South-East Africa	R1	21.47	cor1	0.74
	R2	16.41	cor2	0.79
	R3	11.03	cor3	0.93
Central Africa	R1	27.92	cor1	0.63
	R2	115.49	cor2	0.19
	R3	8.93	cor3	0.98

3.1.7.4 Comparison of Groundwater Recharge Models: Taylor Diagrams Analysis in Different Regions

In this section, we present Taylor diagrams for GWR in all regions (Fig. 13), aiming to comprehensively visualize and evaluate the performance of different models compared to the reference model (CLM5). The diagrams display the standard deviation, correlation coefficient, and root mean squared difference (RMSD) on a single plot. The results indicate a positive correlation between the models and the reference model in all regions, with correlation coefficients ranging from 0.12 to 0.82. Overall, GLDAS exhibits a higher correlation and closer proximity to the reference model compared to ERA5-Land. GLDAS shows correlation values between 0.61 and 0.8, RMSD values between 4.8 and 38, and standard deviation ranging from 3.8 to 68 mm/year. In contrast, ERA5-Land demonstrates a lower correlation, varying from 0.12 to 0.7, RMSD values between 5 and greater than 70, and standard deviation ranging from 1 to greater than 100 mm/year. SAH region stands out with the lowest standard deviation (1 to 3.8 mm/year), RMSD (3.8 to 5), and higher correlation coefficient (0.7 to 0.8) compared to other regions. In MED and SEAF, the models display similar correlation performance, but SEAF exhibits a larger difference in standard deviation between the models compared to MED.

GLDAS performs better in MED and SAH regions in terms of correlation, standard deviation, and RMSD, while performing less well in SEAF. On the other hand, ERA5-Land performs better in SEAF and shows weaker performance in CAF. The Taylor diagrams offer valuable insights into the models' relative performance in different regions, helping to identify regions where specific models excel or require improvement.

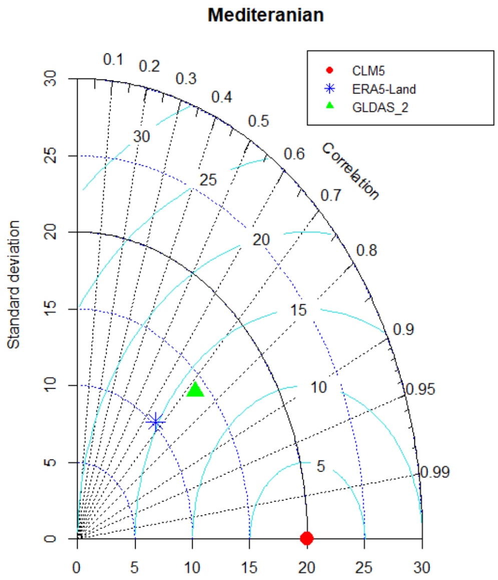

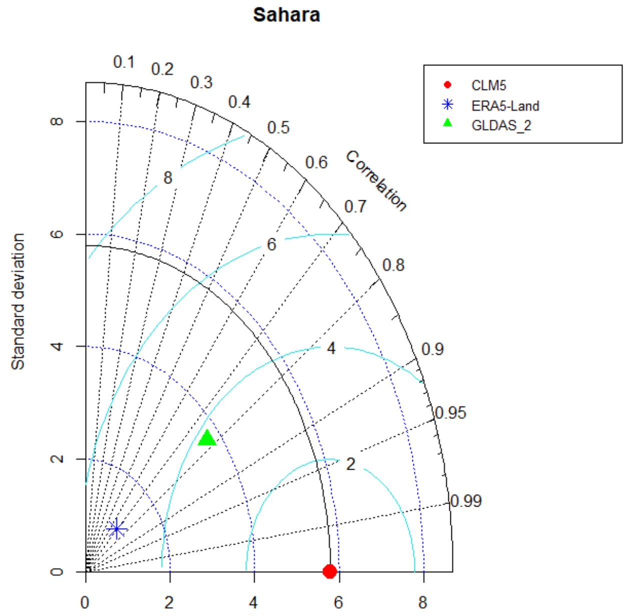

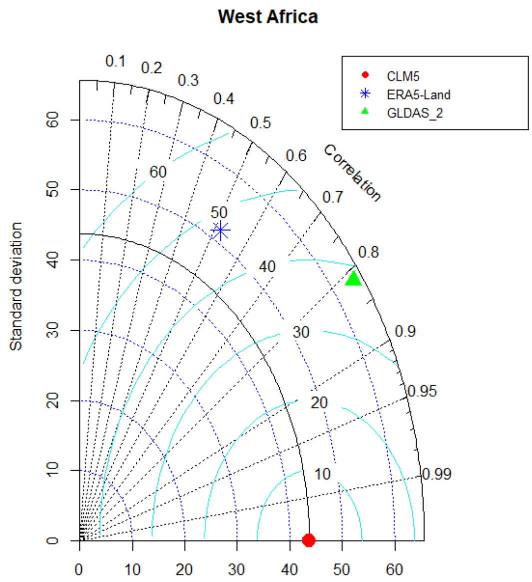

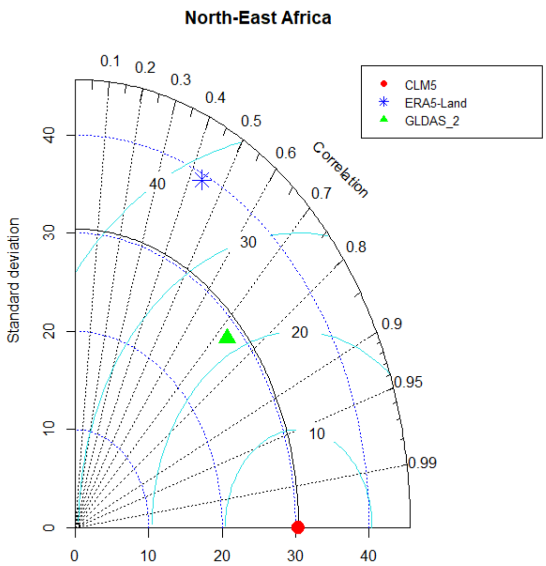

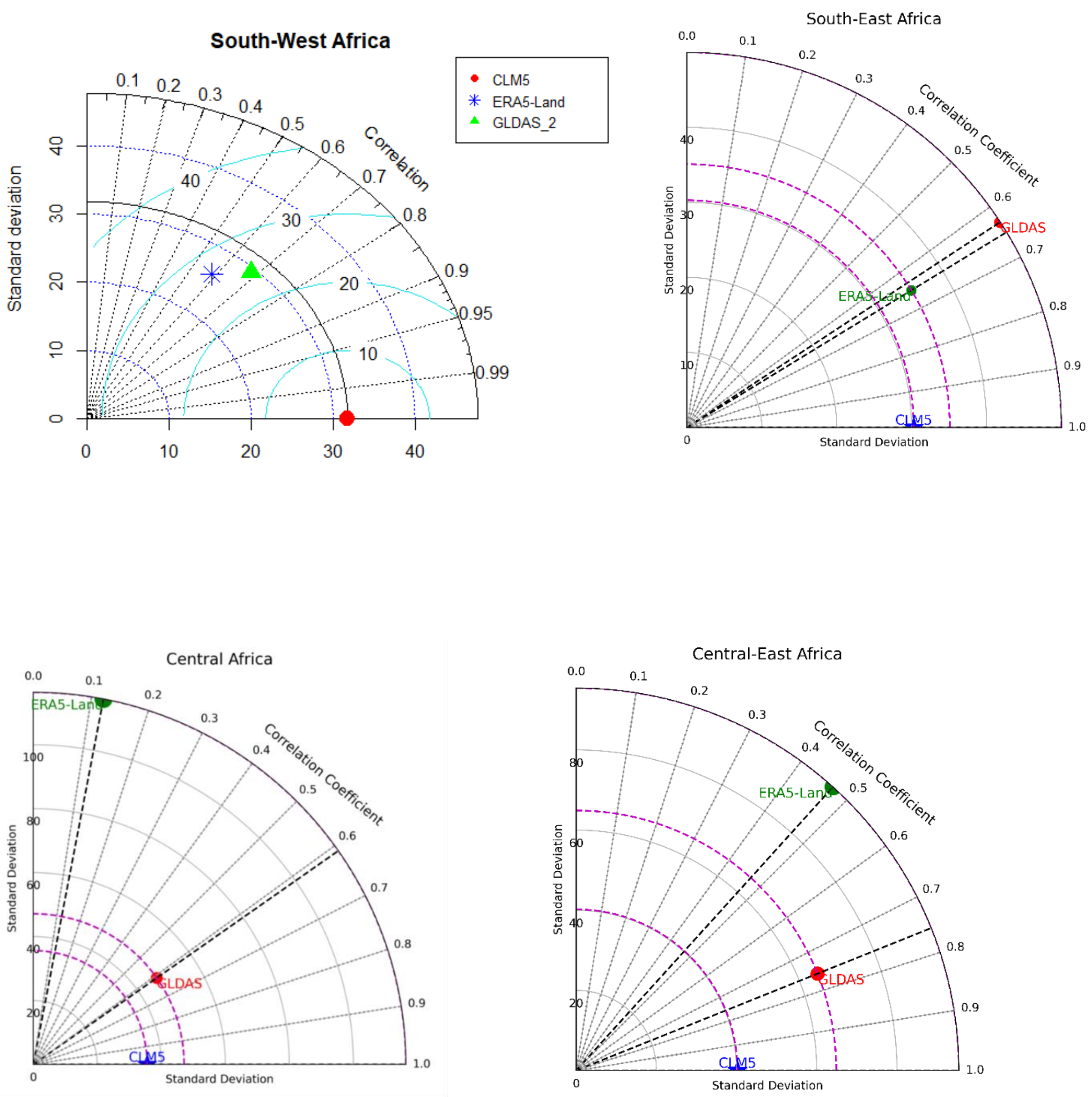

Figure 13. Taylor diagrams for Groundwater Recharge (GWR) showing the relationship and the performance of different dataset compared to the reference (CLM5) in all the regions of study.

3.2 Groundwater Recharge implication for green hydrogen production

There is a growing interest in producing green hydrogen through water electrolysis, powered by renewable electricity sources. This approach is gaining in traction due to the absence of greenhouse gas emissions in renewable electricity generation, making green hydrogen a promising candidate for decarbonizing energy systems, as concluded by Sgobbi et al. (2016). Efficient water electrolysis requires the use of high-purity water, as highlighted by Winter et al. (2022). GWR hold an advantage over other water sources in terms of quality, making them a reliable choice for green hydrogen production. Africa possesses a substantial volume of groundwater, estimated at around 0.66 million km^3, which is 20 times greater than the freshwater stored in African lakes (MacDonald et al., 2021; Springer et al., 2023). Additionally, Africa has renewable groundwater resources of about 2072 km^3/year (Döll and Fiedler, 2008). Considering that producing 1 kilogram of green hydrogen requires about 9 kilograms of water (Beswick et al., 2021), a substantial and good-quality supply of GWR is essential. This study has pinpointed specific regions in Africa, such as CAF, CEAF, WAF, SEAF, and NEAF, where GWR is available and where green hydrogen projects could be economically feasible due to relatively easier GWR extraction. SAH, MED, and SWAF regions hold significant GWR reserves suitable for green hydrogen production. However, due to the deeper groundwater table in these areas compared to other regions, implementing projects there could incur higher costs.

3.3 Limitations of the Approach

This study builds upon models such as CLM5, ERA5-Land, and GLDAS_2.0, which inherently contain assumptions and simplifications. These models rely on specific parameterizations and representations of processes, which might not fully encompass the intricate complexities of real-world hydrological systems. The study's approach involves subtracting ET and Q from PT to estimate the remaining water component, referred to as GWR. However, uncertainties surround this water balance approach. Variations in data inputs among models are an example; the parameterization choices unique to each model can lead to different inputs. Furthermore, the models operate at distinct spatial resolutions: CLM5 at 10 km ERA5-Land at 9 km, and GLDAS_2.0 $\approx$ 28 km. This divergence in spatial resolution may impact the accuracy of results. Moreover, it's important to note that the models might not fully encompass all hydrological processes within the study area. Localized hydrological factors like human activities, land use alterations, and specific geological conditions can influence the water balance, yet might not be comprehensively considered in these models.

PARTIAL CONCLUSION

Within this chapter, our comprehensive analysis allows us to draw several key conclusions. Notably, we observe a pronounced similarity in the spatiotemporal distribution patterns of PT and ET across both models. Particularly, regions encompassing CAF, CEAF, WAF, SEAF, and NEAF prominently exhibit elevated PT and ET availability. However, a noteworthy disparity emerges concerning Q, with GLDAS_2.0 revealing considerably lower values in comparison to CLM5 and ERA5-Land. Turning our attention to Groundwater Recharge (GWR), we discern that GLDAS_2.0 and ERA5-Land depict heightened GWR availability in regions characterized by amplified PT and ET levels. This concurrence emphasizes the interconnectedness of these hydrological variables. Our statistical analyses further reinforce these observations, revealing a strong correlation, particularly pronounced in regions such as the MED, SAH, and SWAF, between CLM5 and GLDAS_2.0. Moreover, the utilization of advanced techniques, including Triple Collocation analysis and the Taylor diagram, serves to accentuate the significance of the relationships and the enhanced accuracy inherent to the datasets.

GENERAL CONCLUSION AND PERSPECTIVES

GENERAL CONCLUSION AND PERSPECTIVES

This study introduces a novel approach, comparing long-term spatial water component distributions to determine groundwater recharge in Africa. The calculated mean decadal groundwater recharge rates are 45.49 mm/year for CLM5, 129.92 mm/year for ERA5-Land, and 155.39 mm/year for GLDAS. Notably, regions like Central Africa, Central-East Africa, West Africa, South-East Africa, and North-East Africa (including Ethiopia) exhibit significant groundwater availability. Robust statistical analysis establishes a strong correlation between CLM5 and GLDAS_2.0, underscoring the impact of precipitation patterns on groundwater recharge dynamics. The role of surface runoff parameterization, considering land conditions, emerges as crucial for accurate surface runoff estimations among models. Interestingly, regions with lower precipitation, such as the Sahara, Mediterranean, and South-West Africa, consistently demonstrate agreement among models. Of particular significance is the accurate assessment of groundwater recharge's role in Africa's green hydrogen production. Groundwater recharge proves pivotal for sustainable green hydrogen generation, a promising clean energy source, particularly amid growing interest in renewable energy solutions for environmental concerns. The study's identification of regions with high groundwater recharge potential serves as a foundation for informed decision-making in establishing green hydrogen projects. Moreover, the findings underscore the necessity of precise hydrological modeling in shaping water resource strategies for sustainable energy development. Future research could prioritize refining surface runoff parameterizations and incorporating localized factors to enhance the precision of groundwater recharge estimations. Additionally, stakeholders and policymakers should collaborate with researchers to assess the feasibility of green hydrogen projects in regions of high recharge potential. This assessment should consider both groundwater availability and the broader renewable energy landscape.

BIBLIOGRAPHY REFERENCES

Abdullateef, L., Tijani, M. N., Nuru, N. A., John, S., & Mustapha, A. (2021). Assessment of groundwater recharge potential in a typical geological transition zone in Bauchi, NE-Nigeria using remote sensing/GIS and MCDA approaches. *Heliyon*, *7*(4), e06762. https://doi.org/10.1016/j.heliyon.2021.e06762

Abiye, T. (2016). Synthesis on groundwater recharge in Southern Africa: A supporting tool for groundwater users. *Groundwater for Sustainable Development*, *2–3*, 182–189. https://doi.org/10.1016/j.gsd.2016.10.002

AbouSeada, N., & Hatem, T. M. (2022). Climate action: Prospects of green hydrogen in Africa. *Energy Reports*, *8*, 3873–3890. https://doi.org/10.1016/j.egyr.2022.02.225

Adelana, M., Macdonald, A., Adelana, S., & Macdonald, A. (2008). Groundwater research issues in Africa. Applied Groundwater Studies in Africa. *IAH Selected Papers on Hydrogeolog*, *13*, 43–64.

Adelana, S. M. A., Taylor, R., Tindimugaya, C., Owor, M., & Shamsudduha, M. (2009). Monitoring groundwater resources in Sub-Saharan Africa: Issues and challenges. *IAHS Red Book Publication*, *334*, 103–113.

Adeleke, O. O., Makinde, V., Eruola, A. O., Dada, O. F., Ojo, A. O., & Aluko, T. J. (2015). Estimation of Groundwater Recharges in Odeda Local Government Area, Ogun State, Nigeria using Empirical Formulae. *Challenges*, *6*(2), 271–281. https://doi.org/10.3390/challe6020271

Akoglu, H. (2018). User’s guide to correlation coefficients. *Turkish Journal of Emergency Medicine*, *18*(3), 91–93. https://doi.org/10.1016/j.tjem.2018.08.001

Alemohammad, S. H., McColl, K. A., Konings, A. G., Entekhabi, D., & Stoffelen, A. (2015). Characterization of precipitation product errors across the United States using multiplicative triple collocation. *Hydrology and Earth System Sciences*, *19*(8), 3489–3503. https://doi.org/10.5194/hess-19-3489-2015

Balek, J. (1988). Groundwater Recharge Concepts. In I. Simmers (Ed.), *Estimation of Natural Groundwater Recharge* (pp. 3–9). Dordrecht: Springer Netherlands. https://doi.org/10.1007/978-94-015-7780-9_1

Balsamo, G., Beljaars, A., Scipal, K., Viterbo, P., Van Den Hurk, B., Hirschi, M., & Betts, A. K. (2009). A Revised Hydrology for the ECMWF Model: Verification from Field Site to Terrestrial Water Storage and Impact in the Integrated Forecast System. *Journal of Hydrometeorology*, *10*(3), 623–643. https://doi.org/10.1175/2008JHM1068.1

Beaudoing, H., & Rodell, M. (2019). GLDAS Noah Land Surface Model L4 monthly 0.25 x 0.25 degree V2.0 (GLDAS_NOAH025_M 2.0) [Research database]. Retrieved June 21, 2023, from GES DISC Dataset website: https://disc.gsfc.nasa.gov/datasets/GLDAS_NOAH025_M_2.0/summary

Beswick, R. R., Oliveira, A. M., & Yan, Y. (2021). Does the Green Hydrogen Economy Have a Water Problem? *ACS Energy Letters*, *6*(9), 3167–3169. https://doi.org/10.1021/acsenergylett.1c01375

Bonsor, H. C., Shamsudduha, M., Marchant, B. P., MacDonald, A. M., & Taylor, R. G. (2018). Seasonal and Decadal Groundwater Changes in African Sedimentary Aquifers Estimated Using GRACE Products and LSMs. *Remote Sensing*, *10*(6), 904. https://doi.org/10.3390/rs10060904

Bouma, J. (1989). Using Soil Survey Data for Quantitative Land Evaluation. In B. A. Stewart (Ed.), *Advances in Soil Science: Volume 9* (pp. 177–213). New York, NY: Springer US. https://doi.org/10.1007/978-1-4612-3532-3_4

Burke, E. J., Brown, S. J., & Christidis, N. (2006). Modeling the Recent Evolution of Global Drought and Projections for the Twenty-First Century with the Hadley Centre Climate Model. *Journal of Hydrometeorology*, *7*(5), 1113–1125. https://doi.org/10.1175/JHM544.1

Calow, R. C., MacDonald, A. M., Nicol, A. L., & Robins, N. S. (2010). Ground Water Security and Drought in Africa: Linking Availability, Access, and Demand. *Groundwater*, *48*(2), 246–256. https://doi.org/10.1111/j.1745-6584.2009.00558.x

Casati, B., Lussana, C., & Crespi, A. (2023). Scale-separation diagnostics and the Symmetric Bounded Efficiency for the inter-comparison of precipitation reanalyses. *International Journal of Climatology*, *43*(5), 2287–2304. https://doi.org/10.1002/joc.7975

Chai, T., & Draxler, R. R. (2014). Root mean square error (RMSE) or mean absolute error (MAE)? – Arguments against avoiding RMSE in the literature. *Geoscientific Model Development*, *7*(3), 1247–1250. https://doi.org/10.5194/gmd-7-1247-2014

Chung, I.-M., Sophocleous, M. A., Mitiku, D. B., & Kim, N. W. (2016). Estimating groundwater recharge in the humid and semi-arid African regions: Review. *Geosciences Journal*, *20*(5), 731–744. https://doi.org/10.1007/s12303-016-0001-5

CLM Technical Note. (2018). Retrieved August 12, 2023, from https://escomp.github.io/ctsm-docs/versions/master/html/tech_note/Introduction/CLM50_Tech_Note_Introduction.html#model-history

CTSM, (2017). CLM Technical Note. [Online]. Available on: https://escomp.github.io/ctsm-docs/versions/master/html/tech_note/index.html. Accessed: August 21, 2023

Cuthbert, M. O., Taylor, R. G., Favreau, G., Todd, M. C., Shamsudduha, M., Villholth, K. G., … Kukuric, N. (2019). Observed controls on resilience of groundwater to climate variability in sub-Saharan Africa. *Nature*, *572*(7768), 230–234. https://doi.org/10.1038/s41586-019-1441-7

Dai, Y., Zeng, X., Dickinson, R. E., Baker, I., Bonan, G. B., Bosilovich, M. G., … Yang, Z.-L. (2003). The Common Land Model. *Bulletin of the American Meteorological Society*, *84*(8), 1013–1024. https://doi.org/10.1175/BAMS-84-8-1013

Danielopol, D. L., Griebler, C., Gunatilaka, A., & Notenboom, J. (2003). Present state and future prospects for groundwater ecosystems. *Environmental Conservation*, *30*(2), 104–130. https://doi.org/10.1017/S0376892903000109

Denager, T., Sonnenborg, T. O., Looms, M. C., Bogena, H., & Jensen, K. H. (2023). Point-scale multi-objective calibration of the Community Land Model (version 5.0) using in situ observations of water and energy fluxes and variables. *Hydrology and Earth System Sciences*, *27*(14), 2827–2845. https://doi.org/10.5194/hess-27-2827-2023

Dieulin, C., Mahé, G., Paturel, J.-E., Ejjiyar, S., Tramblay, Y., Rouché, N., & EL Mansouri, B. (2019). A New 60-Year 1940/1999 Monthly-Gridded Rainfall Data Set for Africa. *Water*, *11*(2), 387. https://doi.org/10.3390/w11020387

Döll, P., & Fiedler, K. (2008). Global-scale modeling of groundwater recharge. *Hydrology and Earth System Sciences*, *12*(3), 863–885. https://doi.org/10.5194/hess-12-863-2008

Dregne, H. E. (Ed.). (1976). Chapter 4 Africa. In *Developments in Soil Science* (pp. 51–70). Elsevier. https://doi.org/10.1016/S0166-2481(08)70097-7

ECMWF. (2018). IFS Documentation CY45R1 - Part IV: Physical processes [Text]. Retrieved September 13, 2023, from ECMWF website: https://www.ecmwf.int/en/elibrary/80895-ifs-documentation-cy45r1-part-iv-physical-processes

Edmunds, W. M., & Gaye, C. B. (1994). Estimating the spatial variability of groundwater recharge in the Sahel using chloride. *Journal of Hydrology*, *156*(1), 47–59. https://doi.org/10.1016/0022-1694(94)90070-1

Entisols | Soil & Water Systems | University of Idaho [Educational]. (2023). Retrieved July 13, 2023, from The Twelve Soil Orders Available on: https://www.uidaho.edu/cals/soil-orders/entisols

European Commission. Joint Research Centre. (2013a). *Soil atlas of Africa.* LU: Publications Office. Retrieved July 13, 2023. Retrieved from https://data.europa.eu/doi/10.2788/52319

European Commission. Joint Research Centre. (2013b). Soil atlas of Africa. [Databased]. Retrieved July 13, 2023, from Soil Atlas of Africa and its associated Soil Map (data) website: https://data.europa.eu/doi/10.2788/52319

Foster, S., & MacDonald, A. (2014). The 'water security' dialogue: Why it needs to be better informed about groundwater. *Hydrogeology Journal*, *22*(7), 1489–1492. https://doi.org/10.1007/s10040-014-1157-6

Gaye, C. B., & Tindimugaya, C. (2018). Review: Challenges and opportunities for sustainable groundwater management in Africa. *Hydrogeology Journal*, *27*, 1–12. https://doi.org/10.1007/s10040-018-1892-1

Gee, G. W., & Or, D. (2002). 2.4 Particle-Size Analysis. In *Methods of Soil Analysis* (pp. 255–293). John Wiley & Sons, Ltd. https://doi.org/10.2136/sssabookser5.4.c12

GSWP3, (2014). Global Soil Wetness Project Phase 3. [Online]. Available on: http://hydro.iis.u-tokyo.ac.jp/GSWP3/index.html. Accessed: August 21, 2023

Guiraud, R. (1988). L'hydrogéologie de l'Afrique. *Journal of African Earth Sciences (and the Middle East)*, *7*(3), 519–543. https://doi.org/10.1016/0899-5362(88)90043-7

Hendrickx, J. M. H. (1992). Groundwater Recharge. A Guide to Understanding and Estimating Natural Recharge (Volume 8, International Contributions to Hydrogeology). *Journal of Environmental Quality*, *21*(3), 512–512. https://doi.org/10.2134/jeq1992.00472425002100030036x

Huang, Z., Yuan, X., & Liu, X. (2021). The key drivers for the changes in global water scarcity: Water withdrawal versus water availability. *Journal of Hydrology*, *601*, 126658. https://doi.org/10.1016/j.jhydrol.2021.126658

Hulme, M. (1992a). A 1951–80 global land precipitation climatology for the evaluation of general circulation models. *Climate Dynamics*, *7*(2), 57–72. https://doi.org/10.1007/BF00209609

Hulme, M. (1992b). Rainfall changes in Africa: 1931–1960 to 1961–1990. *International Journal of Climatology*, *12*(7), 685–699. https://doi.org/10.1002/joc.3370120703

IPCC, I. P. on C. (2007). *Climate Change 2007 - The Physical Science Basis: Working Group I Contribution to the Fourth Assessment Report of the IPCC*. Cambridge University Press.

Iturbide, M., Gutiérrez, J. M., Alves, L. M., Bedia, J., Cerezo-Mota, R., Cimadevilla, E., … Vera, C. S. (2020). An update of IPCC climate reference regions for subcontinental analysis of climate model data: Definition and aggregated datasets. *Earth System Science Data*, *12*(4), 2959–2970. https://doi.org/10.5194/essd-12-2959-2020

Keese, K. E., Scanlon, B. R., & Reedy, R. C. (2005). Assessing controls on diffuse groundwater recharge using unsaturated flow modeling. *Water Resources Research*, *41*(6). https://doi.org/10.1029/2004WR003841

King, L. (1978). The geomorphology of central and southern Africa. In M. J. A. Werger (Ed.), *Biogeography and Ecology of Southern Africa* (pp. 1–17). Dordrecht: Springer Netherlands. https://doi.org/10.1007/978-94-009-9951-0_1

Kumar, C. P. (1997). Estimation of Natural Ground Water Recharge. *ISH Journal of Hydraulic Engineering*, *3*(1), 61–74. https://doi.org/10.1080/09715010.1997.10514603

Lawrence, D. M., Fisher, R. A., Koven, C. D., Oleson, K. W., Swenson, S. C., Bonan, G., … Zeng, X. (2019). The Community Land Model Version 5: Description of New Features, Benchmarking, and Impact of Forcing Uncertainty. *Journal of Advances in Modeling Earth Systems*, *11*(12), 4245–4287. https://doi.org/10.1029/2018MS001583

Lawrence, P. J., & Chase, T. N. (2007). Representing a new MODIS consistent land surface in the Community Land Model (CLM 3.0). *Journal of Geophysical Research: Biogeosciences*, *112*(G1). https://doi.org/10.1029/2006JG000168

Li, H., Liu, G., Han, C., Yang, Y., & Chen, R. (2022). *Quantifying the Trends and Variations in the Frost-Free Period and the Number of Frost Days across China under Climate Change Using ERA5-Land Reanalysis Dataset*. *14*(10), 2400. https://doi.org/10.3390/rs14102400

Liang, X., Lettenmaier, D. P., Wood, E. F., & Burges, S. J. (1994). A simple hydrologically based model of land surface water and energy fluxes for general circulation models. *Journal of Geophysical Research: Atmospheres*, *99*(D7), 14415–14428. https://doi.org/10.1029/94JD00483

MacDonald, A. M., Bonsor, H. C., Dochartaigh, B. É. Ó., & Taylor, R. G. (2012). Quantitative maps of groundwater resources in Africa. *Environmental Research Letters*, *7*(2), 024009. https://doi.org/10.1088/1748-9326/7/2/024009

MacDonald, A. M., & Calow, R. C. (2009). Developing groundwater for secure rural water supplies in Africa. *Desalination*, *248*(1–3), 546–556. https://doi.org/10.1016/j.desal.2008.05.100

Macdonald, A. M., Calow, R. C., Macdonald, D. M. J., Darling, W. G., & Dochartaigh, B. É. Ó. (2009). What impact will climate change have on rural groundwater supplies in Africa? *Hydrological Sciences Journal*, *54*(4), 690–703. https://doi.org/10.1623/hysj.54.4.690

MacDonald, A. M., & Davies, J. (2000). *A brief review of groundwater for rural water supply in sub-Saharan Africa* (Publication - Report No. WC/00/33; p. 30). Nottingham: British Geological Survey. Retrieved from British Geological Survey website: https://nora.nerc.ac.uk/id/eprint/501047/

MacDonald, Alan M., Lark, R. M., Taylor, R. G., Abiye, T., Fallas, H. C., Favreau, G.,West, C. (2021). Mapping groundwater recharge in Africa from ground observations and implications for water security. *Environmental Research Letters*, *16*(3), 034012. https://doi.org/10.1088/1748-9326/abd661

Marshall, M., Funk, C., & Michaelsen, J. (2012). Examining evapotranspiration trends in Africa. *Climate Dynamics*, *38*(9), 1849–1865. https://doi.org/10.1007/s00382-012-1299-y

Martinsen, G., Bessiere, H., Caballero, Y., Koch, J., Collados-Lara, A. J., Mansour, M., Stisen, S. (2022). Developing a pan-European high-resolution groundwater recharge map – Combining satellite data and national survey data using machine learning. *Science of The Total Environment*, *822*, 153464. https://doi.org/10.1016/j.scitotenv.2022.153464

Mileham, L., Taylor, R., Thompson, J., Todd, M., & Tindimugaya, C. (2008). Impact of rainfall distribution on the parameterisation of a soil-moisture balance model of groundwater recharge in equatorial Africa. *Journal of Hydrology*, *359*(1), 46–58. https://doi.org/10.1016/j.jhydrol.2008.06.007

Moe, C. L., & Rheingans, R. D. (2006). Global challenges in water, sanitation and health. *Journal of Water and Health*, *4*(S1), 41–57. https://doi.org/10.2166/wh.2006.0043

Mulyadi, A., Dede, M., & Widiawaty, M. A. (2020). Spatial interaction of groundwater and surface topographic using geographically weighted regression in built-up area. *IOP Conference*

Series: Earth and Environmental Science, *477*(1), 012023. https://doi.org/10.1088/1755-1315/477/1/012023

Muñoz Sabater, J. (2019). ERA5-Land hourly data from 1950 to present [Research database]. Retrieved June 1, 2023, from Copernicus Climate Change Service (C3S) Climate Data Store website:
https://cds.climate.copernicus.eu/cdsapp#!/dataset/10.24381/cds.e2161bac?tab=overview

Muñoz-Sabater, J., Dutra, E., Agustí-Panareda, A., Albergel, C., Arduini, G., Balsamo, G., Thépaut, J.-N. (2021). ERA5-Land: A state-of-the-art global reanalysis dataset for land applications. *Earth System Science Data*, *13*, 4349–4383. https://doi.org/10.5194/essd-13-4349-2021

NASA, (2022). README Document for NASA GLDAS Version 2 Data Products. [Online]. Available on:
https://hydro1.gesdisc.eosdis.nasa.gov/data/GLDAS/GLDAS_NOAH025_M.2.0/doc/README_GLDAS2.pdf. Accessed: August 21, 2023

Nicholson, S. E. (2000). The nature of rainfall variability over Africa on time scales of decades to millenia. *Global and Planetary Change*, *26*(1), 137–158. https://doi.org/10.1016/S0921-8181(00)00040-0

Niu, G.-Y., Yang, Z.-L., Dickinson, R. E., & Gulden, L. E. (2005). A simple TOPMODEL-based runoff parameterization (SIMTOP) for use in global climate models. *Journal of Geophysical Research: Atmospheres*, *110*(D21). https://doi.org/10.1029/2005JD006111

Niu, G.-Y., Yang, Z.-L., Mitchell, K. E., Chen, F., Ek, M. B., Barlage, M., Xia, Y. (2011). The community Noah land surface model with multiparameterization options (Noah-MP): 1. Model description and evaluation with local-scale measurements. *Journal of Geophysical Research: Atmospheres*, *116*(D12). https://doi.org/10.1029/2010JD015139

Nogueira, M., Albergel, C., Boussetta, S., Johannsen, F., Trigo, I. F., Ermida, S. L., Dutra, E. (2020). Role of vegetation in representing land surface temperature in the CHTESSEL (CY45R1) and SURFEX-ISBA (v8.1) land surface models: A case study over Iberia. *Geoscientific Model Development*, *13*(9), 3975–3993. https://doi.org/10.5194/gmd-13-3975-2020

Nogueira, M., Boussetta, S., Balsamo, G., Albergel, C., Trigo, I. F., Johannsen, F., Dutra, E. (2021). Upgrading Land-Cover and Vegetation Seasonality in the ECMWF Coupled System: Verification With FLUXNET Sites, METEOSAT Satellite Land Surface Temperatures, and ERA5 Atmospheric Reanalysis. *Journal of Geophysical Research: Atmospheres*, *126*(15), e2020JD034163. https://doi.org/10.1029/2020JD034163

Obuobie, E. (2008). *Estimation of groundwater recharge in the context of future climate change in the White Volta River Basin, West Africa* (PhD, Universitäts- und Landesbibliothek Bonn). Universitäts- und Landesbibliothek Bonn, Bonn. 153p. Retrieved from https://bonndoc.ulb.uni-bonn.de/xmlui/handle/20.500.11811/3712

Oki, T., & Kanae, S. (2006). Global Hydrological Cycles and World Water Resources. *Science*, *313*(5790), 1068–1072. https://doi.org/10.1126/science.1128845

Qi, W., Liu, J., Yang, H., Zhu, X., Tian, Y., Jiang, X., Feng, L. (2020). Large Uncertainties in Runoff Estimations of GLDAS Versions 2.0 and 2.1 in China. *Earth and Space Science*, *7*(1), e2019EA000829. https://doi.org/10.1029/2019EA000829

Reinecke, R., Müller Schmied, H., Trautmann, T., Andersen, L. S., Burek, P., Flörke, M., Döll, P. (2021). Uncertainty of simulated groundwater recharge at different global warming levels: A global-scale multi-model ensemble study. *Hydrology and Earth System Sciences*, *25*(2), 787–810. https://doi.org/10.5194/hess-25-787-2021

Rodell, M., Houser, P. R., Jambor, U., Gottschalck, J., Mitchell, K., Meng, C.-J., Toll, D. (2004). The Global Land Data Assimilation System. *Bulletin of the American Meteorological Society*, *85*(3), 381–394. https://doi.org/10.1175/BAMS-85-3-381

Rushton, K. R., & Ward, C. (1979). The estimation of groundwater recharge. *Journal of Hydrology*, *41*(3–4), 345–361. https://doi.org/10.1016/0022-1694(79)90070-2

Saxton, K. E., & Rawls, W. J. (2006). Soil Water Characteristic Estimates by Texture and Organic Matter for Hydrologic Solutions. *Soil Science Society of America Journal*, *70*(5), 1569–1578. https://doi.org/10.2136/sssaj2005.0117

Scanlon, B. R., Keese, K. E., Flint, A. L., Flint, L. E., Gaye, C. B., Edmunds, W. M., & Simmers, I. (2006). Global synthesis of groundwater recharge in semiarid and arid regions. *Hydrological Processes*, *20*(15), 3335–3370. https://doi.org/10.1002/hyp.6335

Scanlon, B. R., Rateb, A., Anyamba, A., Kebede, S., MacDonald, A. M., Shamsudduha, M., … Xie, H. (2022). Linkages between GRACE water storage, hydrologic extremes, and climate teleconnections in major African aquifers. *Environmental Research Letters*, *17*(1), 014046. https://doi.org/10.1088/1748-9326/ac3bfc

Schober, P., Boer, C., & Schwarte, L. A. (2018). Correlation Coefficients: Appropriate Use and Interpretation. *Anesthesia & Analgesia*, *126*(5), 1763. https://doi.org/10.1213/ANE.0000000000002864

Seddon, D. (2019). The Climate Controls and Process of Groundwater Recharge in a Semi-Arid Tropical Environment: Evidence from the *Makutapora* Basin, Tanzania. Doctoral Thesis, UCL (University College London), London, 147p.

Sgobbi, A., Nijs, W., De Miglio, R., Chiodi, A., Gargiulo, M., & Thiel, C. (2016). How far away is hydrogen? Its role in the medium and long-term decarbonisation of the European energy system. *International Journal of Hydrogen Energy*, *41*(1), 19–35. https://doi.org/10.1016/j.ijhydene.2015.09.004

Shi, X., Mao, J., Thornton, P. E., & Huang, M. (2013). Spatiotemporal patterns of evapotranspiration in response to multiple environmental factors simulated by the Community Land Model. *Environmental Research Letters*, *8*(2), 024012. https://doi.org/10.1088/1748-9326/8/2/024012

Sibanda, T., Nonner, J., & Uhlenbrook, S. (2009). Comparison of groundwater recharge estimation methods for the semi-arid Nyamandhlovu area, Zimbabwe. *Hydrogeology Journal*, *17*, 1427–1441. https://doi.org/10.1007/s10040-009-0445-z

Springer, A., Lopez, T., Owor, M., Frappart, F., & Stieglitz, T. (2023). The Role of Space-Based Observations for Groundwater Resource Monitoring over Africa. *Surveys in Geophysics*, *44*(1), 123–172. https://doi.org/10.1007/s10712-022-09759-4

Stoffelen, A. (1998). Toward the true near-surface wind speed: Error modeling and calibration using triple collocation. *Journal of Geophysical Research: Oceans*, *103*(C4), 7755–7766. https://doi.org/10.1029/97JC03180

Taylor, R. G., Todd, M. C., Kongola, L., Maurice, L., Nahozya, E., Sanga, H., & MacDonald, A. M. (2013). Evidence of the dependence of groundwater resources on extreme rainfall in East Africa. *Nature Climate Change*, *3*(4), 374–378. https://doi.org/10.1038/nclimate1731

Teklebirhan, A., Dessie, N., & Tesfamichael, G. (2012). Groundwater Recharge, Evapotranspiration and Surface Runoff Estimation Using WetSpass Modeling Method in Illala Catchment, Northern Ethiopia. *Momona Ethiopian Journal of Science*, *4*(2), 96–110. https://doi.org/10.4314/mejs.v4i2.80119

Tsanni, A., & Nakweya, G. (2022). Can groundwater improve water security in Africa? *Nature Africa*, *20*(10), 3819–3837. https://doi.org/10.1038/d44148-022-00140-6

UNICEF, (2022). Africa to drastically accelerate progress on water, sanitation and hygiene – report. [Online]. Available on: https://www.unicef.org/senegal/en/press-releases/africa-drastically-accelerate-progress-water-sanitation-and-hygiene-report. Accessed: August 21, 2023

University of Idaho, (2023). The Twelve Soil Order [Online]. Available on: https://www.uidaho.edu/cals/soil-orders/entisols. Accessed: July 20, 2023

Vizy, E. K., & Cook, K. H. (2002). Development and application of a mesoscale climate model for the tropics: Influence of sea surface temperature anomalies on the West African monsoon. *Journal of Geophysical Research: Atmospheres*, *107*(D3), ACL 2-1-ACL 2-22. https://doi.org/10.1029/2001JD000686

Voudouri, K. A., Ntona, M. M., & Kazakis, N. (2023). Snowfall Variation in Eastern Mediterranean Catchments. *Remote Sensing*, *15*(6), 1596. https://doi.org/10.3390/rs15061596

Wang, L., O Dochartaigh, B., & Macdonald, D. (2010). *A literature review of recharge estimation and groundwater resource assessment in Africa* (Internal Report No. IR/10/051). British Geological Survey. https://doi.org/10/051)

Weerasinghe, I., Bastiaanssen, W., Mul, M., Jia, L., & van Griensven, A. (2020). Can we trust remote sensing evapotranspiration products over Africa? *Hydrology and Earth System Sciences*, *24*(3), 1565–1586. https://doi.org/10.5194/hess-24-1565-2020

West, C., Reinecke, R., Rosolem, R., MacDonald, A. M., Cuthbert, M. O., & Wagener, T. (2023). Ground truthing global-scale model estimates of groundwater recharge across Africa.

Science of The Total Environment, *858*, 159765. https://doi.org/10.1016/j.scitotenv.2022.159765

Wijnen, M., Barghouti, S., Cobbing, J., Hiller, B., & Torquebiau, R. (2018). *Assessment of Groundwater Challenges & Opportunities in Support of Sustainable Development in Sub-Saharan Africa* (p. 160). Washington: World Bank Group. Retrieved from World Bank Group website: https://documents1.worldbank.org/curated/en/420291533931251279/pdf/Assessment-of-groundwater-challenges-and-opportunities-in-Sub-Saharan-Africa.pdf

Wild, A., Chua, Z.-W., & Kuleshov, Y. (2022). Triple Collocation Analysis of Satellite Precipitation Estimates over Australia. *Remote Sensing*, *14*(11), 2724. https://doi.org/10.3390/rs14112724

Winter, L. R., Cooper, N. J., Lee, B., Patel, S. K., Wang, L., & Elimelech, M. (2022). Mining Nontraditional Water Sources for a Distributed Hydrogen Economy. *Environmental Science & Technology*, *56*(15), 10577–10585. https://doi.org/10.1021/acs.est.2c02439

Wright, E. P. (1992). The hydrogeology of crystalline basement aquifers in Africa. *Geological Society, London, Special Publications*, *66*(1), 1–27. https://doi.org/10.1144/GSL.SP.1992.066.01.01

Xu, Y., & Beekman, H. E. (2019). Review: Groundwater recharge estimation in arid and semi-arid southern Africa. *Hydrogeology Journal*, *27*(3), 929–943. https://doi.org/10.1007/s10040-018-1898-8

Yilmaz, M. T., & Crow, W. T. (2014). Evaluation of Assumptions in Soil Moisture Triple Collocation Analysis. *Journal of Hydrometeorology*, *15*(3), 1293–1302. https://doi.org/10.1175/JHM-D-13-0158.1

Zeng, Z., Piao, S., Lin, X., Yin, G., Peng, S., Ciais, P., & Myneni, R. B. (2012). Global evapotranspiration over the past three decades: Estimation based on the water balance equation combined with empirical models. *Environmental Research Letters*, *7*(1), 014026. https://doi.org/10.1088/1748-9326/7/1/014026